THESIS FOR THE DEGREE OF LICENTIATE OF ENGINEERING

Development and application of techniques for predicting and analysing phonon-derived materials properties

Fredrik Eriksson

Department of Physics
CHALMERS UNIVERSITY OF TECHNOLOGY
Göteborg, Sweden 2022

Development and application of techniques for
predicting and analysing phonon-derived materials properties
Fredrik Eriksson

Department of Physics
Chalmers University of Technology
se-412 96 Göteborg, Sweden
Telephone +46 (0)31 772 10 00

Cover: Through-plane phonon dispersion of rotationally disordered MoS_2,
© Erik Fransson.

Chalmers digitaltryck
Göteborg, Sweden 2022

Development and application of techniques for predicting and analysing phonon-derived materials properties

Fredrik Eriksson
Department of Physics
Chalmers University of Technology

Abstract

The thermodynamic properties of materials are of great interest for both scientists and engineers. A large contribution to many properties stems from the vibrational motion of the atoms in the material. An understanding of the dynamics of the vibrating atoms is therefore important for many other areas as well, including, e.g., electronic and optical properties. Since many materials of particular technological interest are crystalline, the vibrations can be studied in the framework of lattice dynamics. One of the main challenges in lattice dynamics is to acquire the force constants that describe the atomic interactions. Using crystal symmetries it is possible to reduce and cast this problem to a linear regression problem. This approach has been implemented in the present work in the hiphive package. The force constants (an interatomic potential) can be fitted to forces obtained from, e.g., density functional theory calculations.

Although the problem of linear regression is well studied from a theoretical point of view the number of unknown coefficients in the force constant expansion is typically very large. Obtaining good models from limited data is possible via regularized regression, which has been successfully applied in many areas of physics. However, how well these techniques work in general for practical problems involving force constants is not well understood. By interfacing with the scikit-learn package, here, the hiphive package has been used to explore how well these techniques work in practice. It is found that many concepts from machine (or statistical) learning can be useful in order to predict macroscopic properties and quantify model uncertainties.

Moving beyond the domain of pure lattice dynamics we also studied the thermal conductivity of rotationally disordered layered materials, which feature weak van-der-Waals interactions between the layers. These structures exhibit a remarkably low through-plane thermal conductivity and their dynamic properties can be described as one-dimensional glasses (a property worth further studies). By performing molecular dynamics simulations on state-of-the-art graphical processing units using the Green-Kubo formalism excellent agreement with experiments could be achieved.

Keywords: Force Constants, Molecular Dynamics, Peierls-Boltzmann Transport, Green-Kubo, Lattice Thermal Conductivity

LIST OF APPENDED PAPERS

I **The Hiphive Package for the Extraction of High-Order Force Constants by Machine Learning**.
Fredrik Eriksson, Erik Fransson and Paul Erhart
Advanced Theory and Simulations **2**, 1800184 (2019)
doi: 10.1002/adts.201800184

II **Efficient construction of linear models in materials modeling and applications to force constant expansions**.
Erik Fransson, Fredrik Eriksson and Paul Erhart
npj Computational Materials **6**, 135 (2020)
doi: 10.1038/s41524-020-00404-5

III **Extremely anisotropic van der Waals thermal conductors**.
Shi En Kim, Fauzia Mujid, Akash Rai, Fredrik Eriksson, Joonki Suh, Preeti Poddar, Ariana Ray, Chibeom Park, Erik Fransson, Yu Zhong, David A. Muller, Paul Erhart, David G. Cahill and Jiwoong Park
Nature **597**, 660–665 (2021)
doi: 10.1038/s41586-021-03867-8

The author's contribution to the papers:

I The author was part of the developing of the software HIPHIVE, in particular the core functionality regarding crystal symmetries and evaluation of the force constant potential. The author wrote most of the paper and performed the simulations except for the Nickel example.

II The author discussed the work and implemented some of the functionality needed in HIPHIVE. Performed the thermal conductivity calculations for the clathrate and proofread the paper.

III The author implemented functionality needed to construct the model system needed for the atomistic modeling. The author wrote the theory part relating to the atomistic modeling and performed the Green-Kubo calculations for predicting the lattice thermal conductivity.

PUBLICATIONS NOT INCLUDED IN THIS THESIS

Efficient Calculation of the Lattice Thermal Conductivity by Atomistic Simulations with Ab Initio Accuracy.
Joakim Brorsson, Arsalan Hashemi, Zheyong Fan, Erik Fransson, Fredrik Eriksson, Tapio Ala-Nissila, Arkady V. Krasheninnikov, Hannu-Pekka Komsa and Paul Erhart
Advanced Theory and Simulation **5**, 2100217 (2022)
doi: 10.1002/adts.202100217

Thermal conductivity in intermetallic clathrates: A first-principles perspective.
Daniel O. Lindroth, Joakim Brorsson, Erik Fransson, Fredrik Eriksson, Anders Palmqvist and Paul Erhart
Physical Review B **100**, 045206 (2019)
doi: 10.1103/PhysRevB.100.045206

Contents

List of abbreviations

ACSF atom-centered symmetry functions. 8

AIC Akaike information criterion. 30, 40

AIMD ab initio molecular dynamics. 5, 10, 23, 26, 27, 34

ARDR automatic relevance determination regression. 29, 40

BCC body-centered cubic. 21

BIC Bayesian information criterion. 30, 40

BO Born-Oppenheimer. 1, 5, 13

BOP bond order potential. 7

CS compressive sensing. 28, 40

DFPT density functional perturbation theory. 18

DFT density functional theory. 1, 3, 5, 6, 14, 18, 23, 25, 40, 43

DOF degree of freedom. 1, 5, 43

EAM embedded atom method. 6

EHM effective harmonic model. 26, 27, 43

EMD equilibrium molecular dynamics. 34, 37

FC force constant. 3, 13–21, 23–28, 32, 39, 40, 43, 44

FCP force constant potential. 3, 15, 23, 27, 39, 43

GAP Gaussian approximation potential. 9

GK Green-Kubo. 3, 31, 34, 36, 43

GP Gaussian process. 8, 9

GPU graphical processing unit. 15

HNEMD homogeneous non-equilibrium molecular dynamics. 36, 37, 41

LASSO least absolute shrinkage and selection operator. 28, 29, 40

LD lattice dynamics. 2, 3, 12, 13, 15, 18, 26, 27

LJ Lennard-Jones. 6

LO-TO longitudinal optic — transverse optic. 18, 19

LTC lattice thermal conductivity. 31, 34

MBTR many-body tensor representation. 9

MC Monte Carlo. 3, 10, 12, 27

MD molecular dynamics. 2, 3, 5, 6, 9, 10, 12, 15, 27, 31, 34, 39

ML machine learning. 3, 5, 7–10, 15, 43, 44

MSE mean squared error. 30

NAC non-analytical correction. 19

NEMD non-equilibrium molecular dynamics. 31, 34

NN neural network. 8, 9, 44

NPT isothermal-isobaric. 10

NVE microcanonical. 10, 31, 34

NVT canonical. 10

OLS ordinary least squares. 3, 14, 18, 27, 40

OMP orthogonal matching pursuit. 29

PBTE Peierls-Boltzmann transport equation. 3, 19, 20, 31–34, 41, 43

PES potential energy surface. 1–3, 5, 8, 15, 16, 19, 25, 27, 29, 32, 39

RFE recursive feature elimination. 29, 30, 40

RMSE root mean squared error. 30, 40

RTA relaxation time approximation. 33

SCHA self-consistent harmonic approximation. 26

SCP self consistent phonons. 26, 43

SMRTA single-mode relaxation time approximation. 33, 34

SOAP smooth overlap of atomic potentials. 8

SSCHA stochastic self-consistent harmonic approximation. 26

TDEP temperature-dependent effective potential. 26

vdW van der Waals. 6, 44

XC exchange-correlation. 2

1

Ab initio modeling of atomic vibrations

Applications rely on materials with specific properties. In order to improve upon old materials and design new ones we must understand why they behave as they do. For a coherent understanding in general we wish to explain their properties from the ground up — from *ab initio*. This means that starting from a microscopic theory based on quantum mechanics we wish to be able to predict macroscopic properties. The study of materials also provide insight into physics in general. While many properties can be understood qualitatively using pen and paper calculations, to get quantitative predictions we must in general use computers. Fortunately, the available computer power has increased exponentially while at the same time advanced algorithms have been developed and become widely available [1–3]. We are now in a position where we can study materials at the atomic scale. This field is commonly known as atomic scale materials modeling. Since it provides a valuable link between theory and reality, the studies are sometimes referred to as computer experiments [4].

This thesis is mainly concerned with the thermodynamic properties associated with the ionic (atomic nuclei) degrees of freedom (DOFs) in materials. This can be motivated by the use of the Born-Oppenheimer (BO) approximation where, for certain properties and materials, the electronic DOFs can be effectively neglected and only the motion of the atomic nuclei are concerned. Thus the atomic nuclei will be modeled as classical or quantum mechanical particles moving around on a potential energy surface (PES) defined by the instantaneous ground state of the electrons. This ab initio PES is often provided by density functional theory (DFT) calculations [5, 6] which is in principle an exact theory without free parameters although in practice approximations must be made. For simplicity, here we will, however, consider the DFT PES as the true PES and our goal is to approximate it as well as we can with minimal effort. However when

comparing to experiments care must be taken as the approximations made, the choice of exchange-correlation (XC) potential, can affect the results.

Now, the starting point of this thesis is the Hamiltonian

$$H = \sum_i \frac{\boldsymbol{p}_i^2}{2m_i} + V_{\mathrm{DFT}}(\boldsymbol{x}) \tag{1.1}$$

of the positions $\boldsymbol{x}_i$ and momenta $\boldsymbol{p}_i$ of the atomic nuclei labeled by i with mass (chemical element) m_i. The function V of the atomic coordinates is called the interatomic potential defining the PES and is the central object we need to understand and work with. The next step is to find a map from this PES to the time dependent phase space distribution function of the system, i.e.,

$$V_{\mathrm{DFT}}(\boldsymbol{x}) \to \rho(\boldsymbol{x}(t), \boldsymbol{p}(t), t). \tag{1.2}$$

The time evolution of the phase space function and the Hamiltonian is commonly carried out via molecular dynamics (MD) simulations, which are the topic of Chapter 2. The field dealing with atomic motion and vibrations in a crystal is called lattice dynamics (LD) and is the topic of Chapter 3. By using, e.g., MD or LD we get access to the dynamics of the system in the thermodynamic sense as the phase space function, in principle, determines the macroscopic properties. However, for the ab initio potential V_{DFT} this is in many cases exceedingly expensive (especially in the case of MD simulations) and a simpler interatomic potential V_{model} is used instead

$$V_{\mathrm{DFT}}(\boldsymbol{x}) \to V_{\mathrm{model}}(\boldsymbol{x}) \to \rho(\boldsymbol{x}(t), \boldsymbol{p}(t), t). \tag{1.3}$$

Some examples of such models will be discussed in Chapter 2 and Chapter 3. This model is typically constructed by sampling configurations $(\boldsymbol{x}, \boldsymbol{f})$ (consisting of positions and forces) from the true potential and then using a regression method to fit the (potential part of the) model Hamiltonian (Chapter 4).

$$V_{\mathrm{DFT}}(\boldsymbol{x}) \to (\boldsymbol{x}, \boldsymbol{f}) \to V_{\mathrm{model}}(\boldsymbol{x}) \to \rho(\boldsymbol{x}, \boldsymbol{p}, t), \tag{1.4}$$

where the forces $\boldsymbol{f} = -\nabla_{\boldsymbol{x}} V(\boldsymbol{x})$ are given by the gradient of the potential. Finally for many purposes we need an explicit method to compute macroscopic properties from the time-dependent phase space distribution. In other words, we need a map from the time-dependent phase space distribution to a macroscopic property A, which could for example be the temperature dependent thermal conductivity $\kappa(T)$

$$V_{\mathrm{DFT}}(\boldsymbol{x}) \to (\boldsymbol{x}, \boldsymbol{f}) \to V_{\mathrm{model}}(\boldsymbol{x}) \to \rho(\boldsymbol{x}(t), \boldsymbol{p}(t), t) \to A \tag{1.5}$$

Such methods for computing the thermal conductivity will be discussed in Chapter 5.

We will in turn explore these five concepts where one realization of this procedure could be

$$V_{\mathrm{CX}}(\boldsymbol{x}) \underset{\mathrm{MC}}{\rightarrow} (\boldsymbol{x}, \boldsymbol{f}) \underset{L_2}{\rightarrow} V_{\mathrm{FCP}}(\boldsymbol{x}) \underset{\mathrm{MD}}{\rightarrow} \rho(\boldsymbol{x}(t), \boldsymbol{p}(t), t) \underset{\mathrm{GK}}{\rightarrow} \kappa(\boldsymbol{T}) \tag{1.6}$$

In other words, a Monte Carlo (MC) method (e.g., Metropolis-Hastings [7, 8]) is used to sample the DFT PES where energies and forces are obtained using DFT calculations. Ordinary least squares (OLS) is then used to construct a model in the form of a force constant potential (FCP) from the sampled data. Finally, MD simulations are carried out and the Green-Kubo (GK) method is used to calculate the thermal conductivity from the time correlation functions of the heat current.

One important observation is that if the model V is simple enough, the maps to macroscopic observables are analytically solvable. For example if the model potential is quadratic in the atomic displacements $\boldsymbol{u} = \boldsymbol{x} - \boldsymbol{X}$ away from equilibrium $\boldsymbol{X}$, i.e., the harmonic approximation $V_{\mathrm{model}} \propto \boldsymbol{u}^2$, the system is analytically solvable and expressions exist for many properties of interest. The simple models also provide a framework and language to discuss anharmonic vibrations as discussed in Chapter 3. The art is to choose the method and model carefully to strike a balance between resources needed and accuracy/precision in each step above. This can be highly dependent on the system at hand and the application in mind.

1.1 Outline

We will begin with a general introduction to interatomic potentials and MD simulations in Chapter 2. The concepts of empirical pair and many-body potentials as well as modern machine learning (ML) based potentials are outlined. A general overview of the basics of MD simulations is presented, including ensembles and the ergodic hypothesis.

Next a specific form of an interatomic potential namely the FCP (or force constant (FC) expansion) is presented in Chapter 3. Its basic components such as clusters and orders are discussed as well as symmetries and constraints. Together with the FCP the framework of LD is presented introducing harmonic phonons as a basis for atomic vibrations in a crystal. We will also address how higher order force constants introduce phonon-phonon interaction leading to frequency shifts and finite lifetimes. Briefly the concept of self-consistent phonons will be discussed.

Following that, some methods for sampling the PES to generate fit data will be presented in Chapter 4, together with a brief introduction to regularized regression as a method for combating over-fitting.

Finally in Chapter 5 two methods for thermal conductivity calculations are presented; the LD based Peierls-Boltzmann transport equation (PBTE) and the MD based GK method.

2

Molecular dynamics

MD is a computational technique where the equations of motion for a system of atoms are (numerically) integrated in time. The forces acting on the atoms are computed from some (conservative) force field as the gradient of the interatomic potential with respect to the positions. Since the force is the gradient of the energy with respect to positions the force field is a gradient of a scalar potential, hence the name interatomic potential. For small systems and short time scales it is in principle possible to perform so-called ab initio molecular dynamics (AIMD) simulations in order to analyze the motion of atoms. Then the atomic forces (and other DOFs) are calculated by solving the (electronic) Schrödinger equation and integrating the equations of motion. For large systems this becomes, however, exceedingly expensive due to the poor scaling of DFT calculations (especially with respect to system size, as the cost scales approximately with the cube of the number of electrons). Thus we want to approximate the BO PES with a simple analytical form involving only the positions of the ions[1] in order to study large systems on long time scales. Such an approximation of the PES is captured by an interatomic potential and can be roughly divided into two classes: traditional analytical (or empirical) potentials with comparably few parameters and simple functional forms, and modern, heavily parameterized potentials often incorporating ML techniques in either the construction of the potential or in the functional form itself. We will start this chapter with a brief overview of interatomic potentials and the need for ML potentials and end with an overview of the MD technique.

[1] In MD simulations the terms ions and atoms/atomic nuclei are often used interchangeably

2.1 Analytical potentials

The first serious use of an interatomic potential was perhaps the work of Fermi, Pasta, Ulam, and Tsingou in the 1950ies[9, 10]. They used the newly constructed MANIAC system to study the interactions between particles in a linear chain, a standard problem in solid state physics. The particles were connected by simple harmonic springs with a small anharmonic perturbation and what they found was a surprising recurrence of the phase space path breaking the ergodic hypothesis, a cornerstone of MD.

After the linear chain and other simple systems such as interacting hard spheres, the Lennard-Jones (LJ) [2] liquid was analyzed by computational means in the 1960s. The LJ potential is one of the simplest analytical interatomic interactions and still widely used today. The term analytical potential comes from the possibility to write down an analytical expression for the interaction. The LJ potential consists of a weak attractive part modeling the van der Waals (vdW) interactions and a strong repulsive core modeling the Pauli exclusion principle. The functional form is

$$V(r) = 4\epsilon \left[\left(\frac{\sigma}{r}\right)^{12} - \left(\frac{\sigma}{r}\right)^{6} \right] \tag{2.1}$$

and the potential is plotted in Fig. 2.1. The free parameters σ and ϵ determine the length and the strength of the interaction and are specific for a given system, say Argon or Helium. Despite its simplicity the LJ potential exhibits interesting behavior such as phase transitions.

The LJ potential is a simple example of a pair potential that works well for gases and some liquids, and pair potentials in general are heavily used in generalized vdW theory [11] (also known as classical DFT). Pair potentials are also typically the starting point when deriving expressions for instantaneous (i.e., possible to calculate at a single point in phase space) thermodynamic properties and pair forces. Often the functional form consists of just a few parameters which makes them well behaved in MD simulations. For gases (low density) and liquids (high disorder) two body potentials work well or when the Coulomb pair-interaction dominates in ionic materials.

During the 1970s many systems were investigated using pair potentials such as water, molecules, and even proteins. But in order to describe more complex materials many-body affects must be taken into account. Such models emerged during the 1980ies and include, e.g., embedded atom method (EAM) potentials [12], which can be cast in the form

$$V = \sum_{ij} V_2(r_{ij}) + \sum_{i} F\Big[\sum_{j} \rho(r_{ij}) \Big]. \tag{2.2}$$

Here V_2 is a pair potential and F is called the embedding functional. The form is well suited to model metals where the atoms move in a sea of electrons and the many-body

[2] Named after Sir John Lennard-Jones

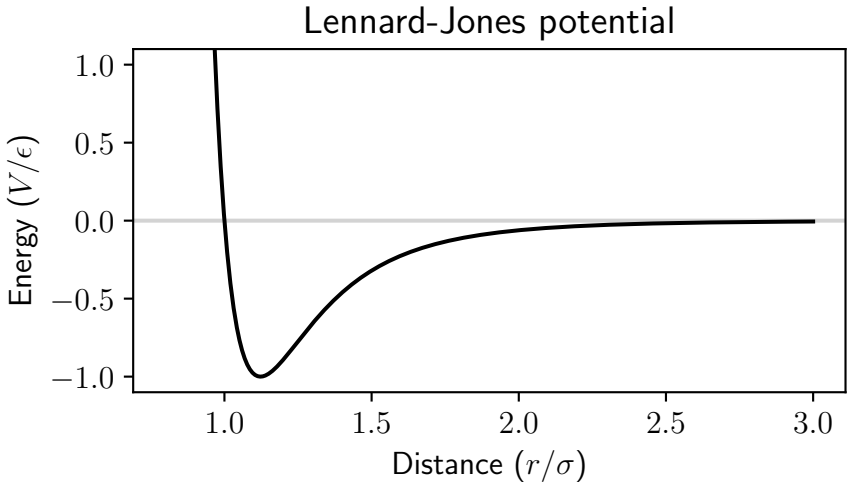

Figure 2.1: The Lennard-Jones potential. To the left of the minimum the strong repulsive part modeling the Pauli exclusion force dominates, while on the right the weak van-der-Waals attractive part dominates. The minimum is located at a distance of $\sqrt[6]{2}\sigma$ where the potential energy is $-\epsilon$. Notice how the potential is nearly zero beyond approximately 3σ.

effects enter as a density dependent two-body interaction ρ. These types of potentials are sometimes called (pair) functionals as they are parameterized via functions instead of real parameters. This idea can be seen as a precursor to the modern types of heavily parameterized potentials.

For more complex molecules or covalently bonded materials such as silicon we need also angular dependence which enters as a "true" three-body effect (e.g., via angles) instead of an aggregated effect such as the density, see Fig. 2.2. One such potential is the bond order potentials (BOPs) developed in the late 1980s by Abell [13] and Tersoff[14]

$$V = \sum_{ij} V_2^R(r_{ij}) + b_{ij} V_2^A(r_{ij}), \tag{2.3}$$

where b_{ij} depends on all angles θ_{ikj}. For more information on analytical potentials see [15].

During the 1990s and 2000s these types of potentials were successfully used for many systems including multi-component systems and also combinations of several types of potentials. However, they are hard to develop and systematically improve. Thus in tandem with faster hardware and development of the ML field new types of potentials emerged during the 2010s which were heavily parameterized with no easy functional form. For more information about the historical development of analytical potentials see [16, 17].

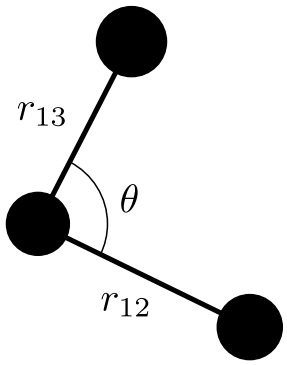

Figure 2.2: A cluster of three atoms described by three parameters, two bond distances and one bond angle. The potential energy $V(r_{12}, r_{13}, \theta)$ is an explicit function of the angle and can in general not be described/decomposed into pure two-body interactions. This model would be suitable for e.g. the internal forces in a water molecule.

2.2 Machine learning potentials

With the growth of the field of ML and the increasing performance of computers another class of potentials has emerged called ML potentials. For a good overview of ML potentials see [18]. The aim is to bridge the gap between pure ab initio methods and analytical potentials. The main problem with analytical potentials is that for complex systems it becomes difficult to construct a suitable functional form to describe all the interactions. The idea behind ML potentials is that a very flexible functional (e.g., neural networks (NNs)[19–21] or Gaussian process (GP) [22, 23]) can be trained given enough data. The drawback with these types of potentials is that the functional form is not easily (if at all) interpretable by a human and thus gives little insight into the underlying physics. Furthermore the parameter landscape is typically vast and care must be taken during the optimization to mitigate both overfitting and underfitting. Finally, these potentials have essentially no extrapolation capacity but should be considered as pure interpolations of the configuration space seen during training. It is thus very important to choose training structures spanning the phase space of interest.

The first part of a ML potential are the descriptors which capture the local environment around an atom and serve as inputs to the functional form instead of the raw atomic coordinates. There are a huge number of atomic descriptors and the challenge is to create descriptors such that the resulting PES obeys relevant global symmetries such as translational and rotational invariance. The construction of (good) descriptors is difficult. They must be simple enough to be fast to calculate but span a complex enough space so that different atomic configurations are discernible. They should also be robust so that similar descriptors represent similar structures. Some examples of atomic descriptors commonly used in materials physics are distances, angles, Coulomb-matrices, smooth overlap of atomic potentials (SOAP), atom-centered symmetry func-

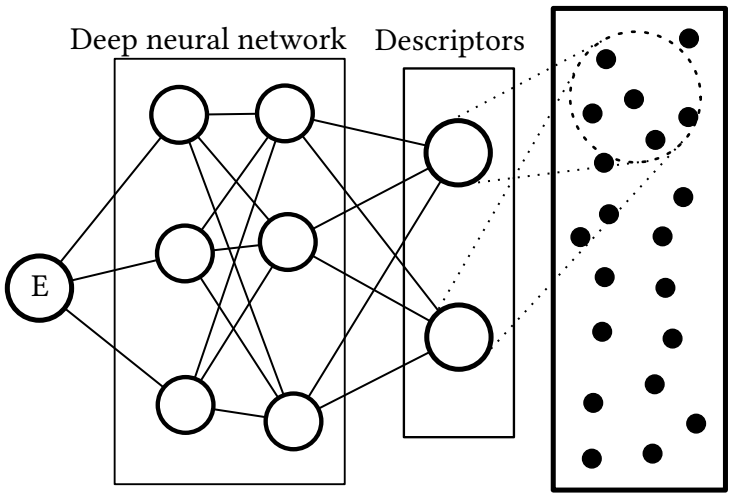

Figure 2.3: Illustration of a machine learning potential. To the right is a configuration of atoms. Two descriptor functions transform the Cartesian coordinates of the neighboring atoms around the atom in the center to suitable input to a deep neural network. The network outputs the energy of the center atom.

tions (ACSF), and many-body tensor representation (MBTR), see, e.g., [24]. Typically the number of descriptors (i.e., the complexity or size of the basis) should be systematically expandable until it is, in principle, possible to reconstruct the original configuration.

The functional form takes the output from the descriptors and calculates the energy (or other properties) of the system, see Fig. 2.3. To be useful for MD purposes derivatives of the descriptors and the functional form must be available in order to calculate forces and virials. The functional form can for example be based on GPs (Gaussian approximation potential (GAP)[22]), NNs[19, 25] or cluster/series expansions [26, 27], but any regression model can in principle be used.

The training method for ML potentials follows the general procedure as outlined in the section about regularized regression Chapter 4 except that non-linear optimization is needed. Typically the functional forms are comparably well understood and the techniques to train them well tested in many fields. Typical methods include stochastic gradient descent, evolutionary algorithms, and maximum likelihood estimation [28].

ML potentials are typically described as interpolation techniques and as such sometimes behave unexpectedly when posed with unseen structures or local environments. Analytical potentials on the other hand are often constructed based on physical insight and only contain a handful of parameters (highly regularized). As a result, they can yield at least somewhat sensible results beyond the training regime. While the choice of descriptors and functional forms as well as optimization techniques are fairly well understood, the selection of training structures is still a rather delicate aspect. Here,

physical intuition and experience play a large role as well as prior understanding of the material at hand. There are various techniques to systematically choose good training data based on active learning and entropy maximization but this is ongoing research [29]. For a nice comparison and discussion of ML potentials see [30].

2.3 Ensembles and the ergodic hypothesis

Sampling the phase space of an interacting many body system is typically done using MC and MD techniques, see, e.g., Frenkel and Smit [31]. MD is the key technique used to model atomic motion in materials as it gives access to time-dependent quantities. The idea is to integrate the equations of motions $\boldsymbol{F} = m\ddot{\boldsymbol{x}}$ (a second order non-linear differential equation) where the force is given as the gradient of the interatomic potential $\boldsymbol{F}_i = -\nabla_{\boldsymbol{x}_i} V(\boldsymbol{x})$ with respect to the atomic positions $\boldsymbol{x}_i$. Many advanced integrators are available that can take multiple steps which can sometimes be useful in AIMD but for practical purposes when dealing with empirical potentials almost always a variant of the Verlet algorithm [4] is used such as velocity Verlet. The most important thing for an integrator is to be able to conserve the energy of the system in order to properly represent the microcanonical (NVE) ensemble. The ergodic hypothesis can then be used to calculate thermodynamic properties via time averages instead of ensemble averages

$$\langle A \rangle = \frac{1}{T} \int_0^T A(t)\, \mathrm{d}t, \tag{2.4}$$

where the angle bracket denotes an ensemble average corresponding to the macroscopic observable A. Limitations of MD include quantum effects and computational cost, MD being somewhat of a brute force approach. The quantum mechanical aspect can to some degree be remedied by using path integral MD [32] but in this case time-correlations are not well defined, whence one cannot extract, e.g., transport coefficients. Fortunately there is a weak relation between temperature and quantum effects and often at low temperatures where quantum effects start to become important other techniques can be used due to the harmonic nature of the potential at low temperatures.

In order to sample other ensembles such as the canonical (NVT) or isothermal-isobaric (NPT) ensembles a thermostat and/or a barostat is needed. These can be based on instantaneous expressions for the thermodynamic properties they try to regulate or on time-averaged properties. In general the temperature is comparably easy to control via, e.g., the equipartition theorem. Typically the integrator is modified in order to incorporate and additional term in the Hamiltonian modeling the heat bath exchanging energy with the system. Care must be taken to have a sufficiently large system so that the effect of the thermostat is comparably weak when sampling dynamical properties. This is motivated by the fact that for large systems the NVE and NVT ensembles are equivalent. Thermostats will appear again later in Chapter 5 during the discussion of

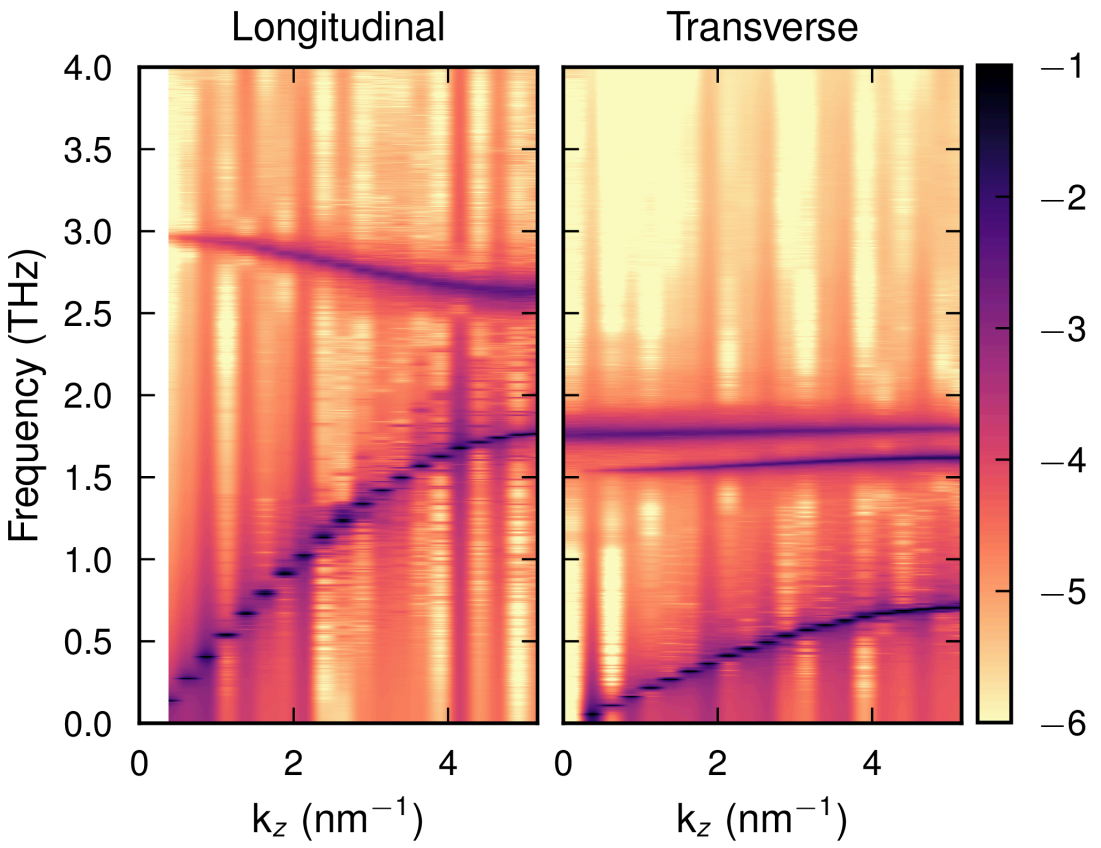

Figure 2.4: Typical dispersion relation calculated using velocity auto-correlation functions. To the left is longitudinal modes where the vibrations are in the direction of the momentum (such as sound waves). To the right are transverse mode with motion perpendicular to the momentum (such as electro-magnetic waves). The acoustic modes originate from the gamma (Γ) point while the optical modes appear as horizontal bands. This example is bulk MoS_2 in the through-plane direction taken from Paper III. The line-width of the dispersion is very thin indicating a harmonic system with long lifetimes. The striped appearance appears since a supercell can only represent a finite number of momentum transfer vectors.

thermal conductivity as they can be used to transport heat or to probe the response function of a system. Commonly used thermostats include the Nosé-Hoover family, the Bussi–Donadio–Parrinello [33] thermostat, and the Langevin thermostat.

Barostats typically require more detailed information about the interatomic potential in question. In principle the instantaneous stress tensor must be calculated which requires the virials, which can be challenging for many-body potentials and when periodic boundary conditions are present [34]. The presence of many-body effects on state variables is in general well understood in terms of hydrodynamic variables but in practice challenging to implement explicitly.

2.4 Time dependence and correlation functions

Many interesting properties are directly accessible from trajectories obtained from MD simulations such as microscopic mechanisms for diffusion of defects [35]. Macroscopic properties of interest such as free energies are more difficult to sample. Typically additional techniques must be used on top of the MD that require many individual simulations at different temperatures, volumes etc. One of the main advantages of the MD technique over MC is that it also gives us the possibility to sample time-dependent properties such as time-correlation functions. In the near-equilibrium limit the fluctuation-dissipation theorem and linear response theory give us direct access to non-equilibrium properties such as thermal conductivities (see Chapter 5) given that suitable observables can be defined. There is also the possibility to sample properties far from equilibrium such as phase transitions.

One important property is the spectral function which can be calculated from the auto-correlation functions of the atomic motion [36, 37]. The spectral function is the dispersion relation of a material and relates the wavelength of lattice waves/phonons to the frequency of the same waves, see Fig. 2.4. This provides us with a method to non-perturbatively sample the dispersion relation and lifetimes/widths of the system that can be compared to results obtained from theoretical methods using LD or to experiments via, e.g., inelastic scattering with neutrons [38] or X-rays.

3

Lattice dynamics

In this chapter first an overview of FCs is presented and then their application in the context of LD is discussed. For FCs suitable sources include the text books by Born and Huang [39], Ziman [40], Choquard [41], Wallace [42] and Srivastava [43].

3.1 Force constant expansions

In order to analyze vibrations in a crystal we need a model Hamiltonian describing the interactions between the atoms. By using the BO approximation we can write the lattice contribution to the energy of the crystal as a Taylor expansion in displacements u around the lattice points $\boldsymbol{R}$,

$$H = K + V = K + E_0 + \Phi_i u_i + \frac{1}{2!}\Phi_{ij} u_i u_j + \frac{1}{3!}\Phi_{ijk} u_i u_j u_k + \dots , \tag{3.1}$$

where $\boldsymbol{K}$ is the kinetic energy of the atoms and Φ are the FCs, named such as they relate energy and displacements. The indices here are compound indices $i = \{\mu, \alpha, \boldsymbol{n}\}$ where μ enumerates the basis of the crystal, α denotes the (Cartesian) direction, and $\boldsymbol{n} \in \mathbb{Z}$ enumerates the primitive cells.

The first coefficient E_0 is the cohesive energy of the crystal. The second term Φ_i is exactly zero if the crystal is in its equilibrium configuration at zero temperature where all forces are zero. The second-order term is the basis for the harmonic analysis of crystals to be discussed later. Third and higher-order terms are referred to as anharmonic terms and play an important role in phase transitions and thermal transport. These concepts are illustrated in Fig. 3.1.

The goal is to find the FC coefficients describing the material in question and then use the above Hamiltonian to calculate properties of interest or to study microscopic

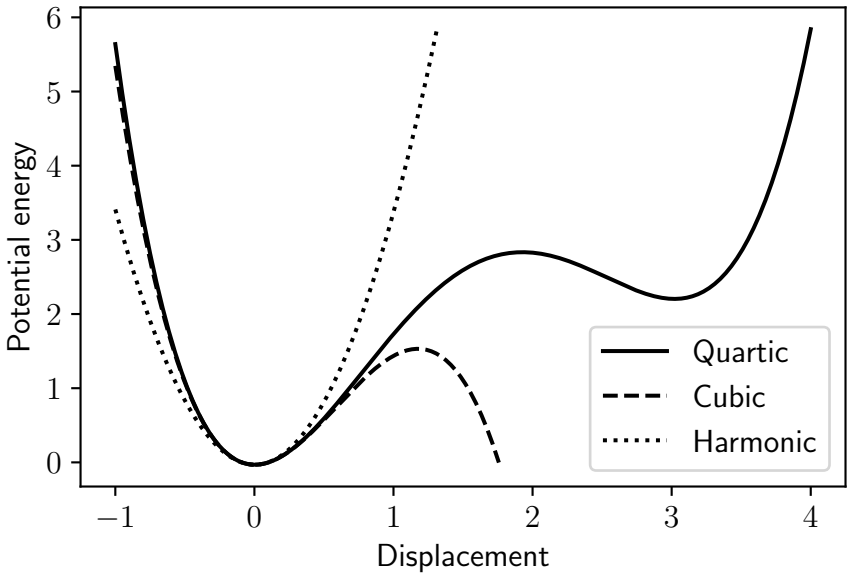

Figure 3.1: Illustration of the potential energy surface of a system. The harmonic approximation is only good for low energies (low temperatures). The cubic correction would improve the description of the landscape close to the origin but makes the potential unstable after about 1 distance unit. The quartic potential stabilizes the surface and are needed in general to describe dynamically stabilized phases.

mechanisms. Notice that this is an interatomic potential that, provided we can find the coefficients, can be systematically improved by increasing the order of the expansion. The force is simply the gradient of the above expansion with respect to the atomic positions

$$F_i = -\frac{\partial V}{\partial u_i} = -\Phi_i - \Phi_{ij} u_j - \frac{1}{2!}\Phi_{ijk} u_j u_k - \dots \tag{3.2}$$

and is still linear in the free parameters (the FCs). Thus, for a fixed set of configurations (displacements) this can be written in matrix form as

$$F_i = U_{ia} \Phi_a, \tag{3.3}$$

where U_{ia} is a matrix mapping for all the displacements and Φ_a is the collection of FCs flattened to an array

$$\Phi_a = [\Phi_0, \Phi_1, \dots, \Phi_N, \Phi_{00}, \Phi_{01}, \dots, \Phi_{NN}, \Phi_{000}, \dots]. \tag{3.4}$$

Thus to find the coefficients we usually use OLS to fit the expansion to ab initio forces calculated using, e.g., DFT.

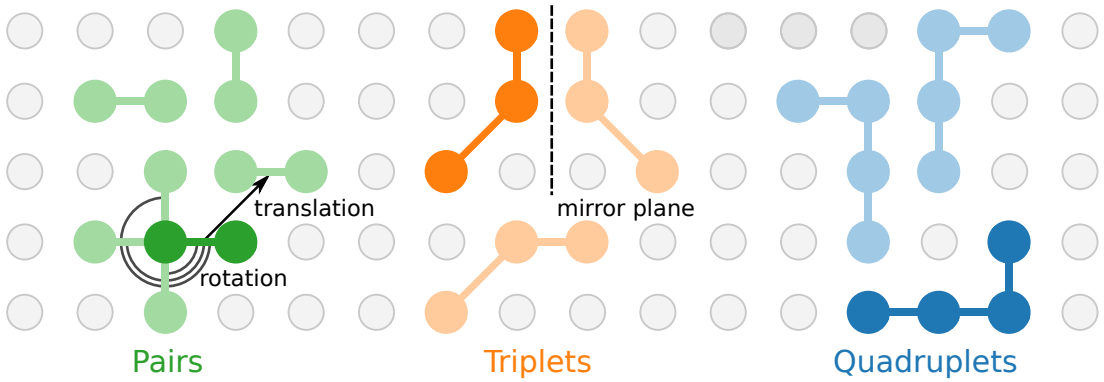

Figure 3.2: Illustration of possible clusters in a lattice system. To each cluster belongs a set of FCs which must obey the lattice symmetries.

However, this expansion must be truncated in some way in order to keep the number of unknown coefficients manageable. First and foremost we cut off the expansion after some order. For harmonic models only second order terms are kept. If we want to study heat transport at least third order terms must be included while dynamically stabilized materials might need fourth order terms to adequately describe the PES.

It is also possible to incorporate our physical intuition that atoms far away from each other only interact weakly. Thus we can view the above expansion as a cluster expansion where each force constant coefficient $\Phi_{ijk\ldots}$ represents a cluster of atoms $(ijk\ldots)$. For example a cluster $(ijkk)$ would be a 3-body, fourth order cluster; see Fig. 3.2 for an illustration of clusters and crystal symmetries. Now we postulate that if two atoms i and j are further away from each other than some cutoff c all FCs where these two atoms are present must be zero, i.e., $\Phi_{\ldots i\ldots j} = 0$. In addition, we know that in general n-body clusters are more important than $n+1$-body clusters and higher orders are typically less important for most applications.

The FCP has advantages and disadvantages compared to other interatomic potentials. It is mathematically well studied and forms the basis of the standard theory of LD. Thus, it makes it straightforward to combine and compare (computer aided) theoretical techniques with direct computer simulations such as MD. The functional form is also simple to implement on, e.g., graphical processing units (GPUs) which, in principle, should make it fast to evaluate for, e.g., MD. There is no limit (other than computer memory and speed) to include larger clusters and higher order thus making the model scalable and tunable. The FC expansion is also linear in the unknown coefficients (the FCs) which makes it easier to analyze and fit compared to ML potentials.

On the other hand, the number of free parameters to determine grows rapidly with increasing anharmonicity (order), range (cutoff), and disorder (number of atoms in the primitive cell) making it difficult to use for, e.g., glasses. The expansion is also firmly

rooted in the lattice and when the PES is shallow and the atoms move far from the lattice points the expansion can quickly become unstable. This can for example happen near a phase transition or when the defect formation energy is low.

Next, the main features of the FC expansion will be presented and what must be taken into account in order to make the extraction of the coefficients feasible in practice.

3.1.1 Crystal symmetries

The crystal lattice imposes certain symmetries on the FCs. For example the equality of mixed partials enforces

$$\Phi_{ij\dots} = \Phi_{P(ij\dots)}, \tag{3.5}$$

where P is any permutation. The crystal/molecular symmetries $S_{i'i}$ impose further conditions on the FCs

$$\Phi_{i'j'\dots} = S_{i'i}S_{j'j}\dots\Phi_{ij\dots} \tag{3.6}$$

along with the translational invariance of the lattice for crystals

$$\Phi(n, n', \dots) = \Phi(n + N, n' + N, \dots), \tag{3.7}$$

where n and N index the primitive cell. Note that they are all expressed as linear constraints and thus relatively easy to handle computationally. All these symmetries are used in HIPHIVE via SPGLIB [44] in order to reduce the number of free parameters. More information can be found in Paper I.

3.1.2 Global symmetries

Apart from the local symmetries the FC expansion must obey some global symmetries namely translational and rotational invariance. These symmetries define so-called sum rules which for the translational invariance take the form

$$\sum_{\mu} \Phi^{\alpha}_{\mu\dots} = 0. \tag{3.8}$$

The translational sum rule ensures that no force acts on the atoms under a translation of the lattice. Note that the Cartesian component has been moved out of the compound index i as the sum has to be fulfilled for all three Cartesian directions independently. The translational sum rule is important for the behavior of the dispersion relation near the Γ point (i.e., at zero momentum) where it should tend to zero for acoustic phonons, see Fig. 3.4.

There are two kinds of rotational sum rules [39, 42]. The (second-order) Born-Huang sum rule reads

$$\sum_{j} \Phi^{\alpha\beta}_{ij} r^{\gamma}_{j} = \sum_{j} \Phi^{\alpha\gamma}_{ij} r^{\beta}_{j} \tag{3.9}$$

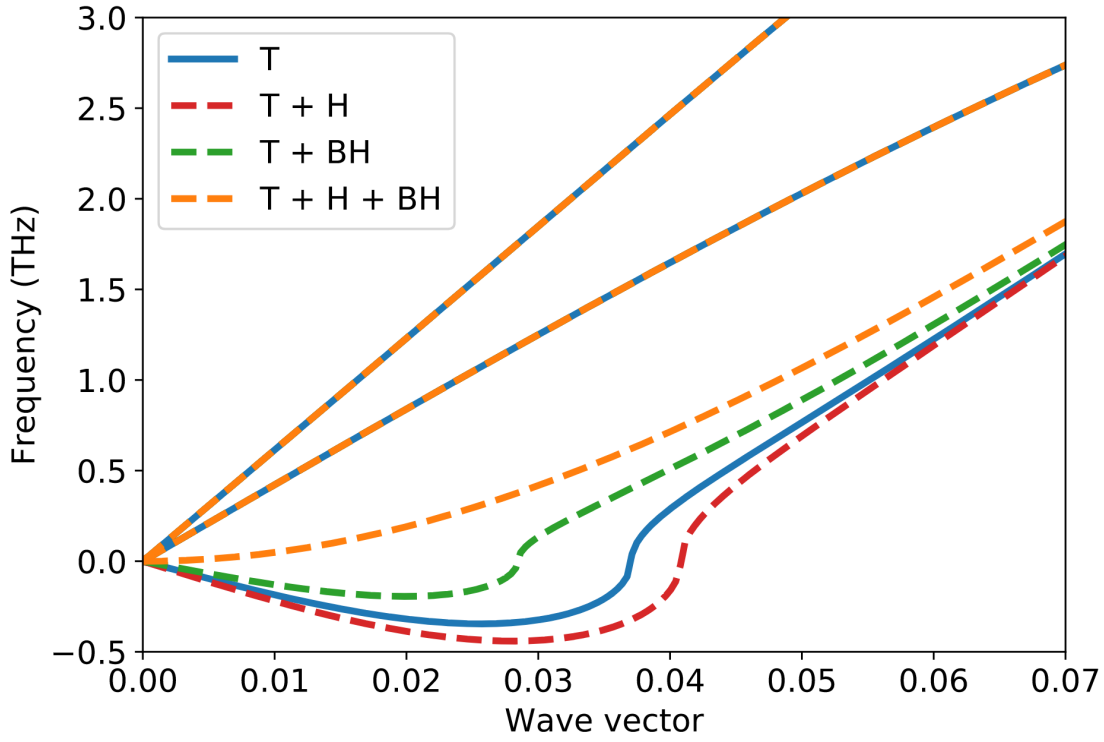

Figure 3.3: Dispersion relation of MoS_2 near the Γ-point (i.e., zero momentum) along the 100 direction. The translational (T) sum rules (3.8) are fulfilled as the dispersion goes to zero at Γ. The Born-Huang (BH) sum rules (3.9) and Huang (H) constraints (3.10) are needed to enforce the correct quadratic behavior of the lowest transverse acoustic mode.

and corresponds to no induced torque under a rotation of the lattice. In general, these sum rules will couple different orders of the expansion to each other but only considering second-order sum rules is sufficient to enforce the quadratic behavior of out-of-plane (ZA) modes in 2D materials [45].

Additionally, there are the Huang constraints enforcing the correct behavior of the elasticity tensor

$$\sum_{ij} \Phi_{ij}^{\alpha\beta} r_i^{\gamma} r_j^{\delta} = \sum_{ij} \Phi_{ij}^{\gamma\delta} r_i^{\alpha} r_j^{\beta}, \tag{3.10}$$

which are important for the elastic constants to exhibit the correct symmetries. The rotational sum rules are especially important in two-dimensional materials, where they are needed to enforce the correct quadratic behavior of the transverse acoustic modes near the Γ-point, see Fig. 3.3.

The two sets of symmetries (crystal and global) define a set of irreducible FCs ϕ where any set of FCs obeying the above symmetries can be written as a linear combination of

the irreducible ones, i.e.,

$$\Phi = \sum_k a_k \phi^k. \tag{3.11}$$

The most straightforward way to extract the new free parameters a from ab initio calculations is to fit them to forces of semi-random (see Chapter 4) configurations using OLS which for the second-order FCs implies

$$F_{ni} = -a_k \phi^k_{ij} u_{nj}, \tag{3.12}$$

where n enumerates the configurations. This approach is sometimes called the regression approach and was introduced by Esfarjani and Stokes in 2008 [46].

3.1.3 Long range corrections

As long as the cutoffs are longer than the expected interactions in the material, the above approach, using cutoffs to limit the number of free parameters, works well. In some cases though there are long-range forces present. This can for example happen in two-dimensional materials where the screening is weaker or in polar materials with large dynamic (Born effective) charges. In these materials the displacements induce a long-ranged electrostatic dipole-dipole interactions [47], which, in theory, have an infinite range. This effect is the reason behind the so called longitudinal optic — transverse optic (LO-TO) splitting where the longitudinal optical (LO) and transverse optic (TO) modes have a seemingly non-analytical behavior near the Γ-point [48], see Fig. 3.4. This can be effectively remedied using the technique introduced by Gonze and Lee [49, 50] and the dispersion can be corrected around the Γ-point. It is important to remember that if the FCs are constructed in a finite periodic supercell and all FCs are included, the corresponding dispersion is correct at supported inverse lattice points [51]. If the FCs are long-ranged the Fourier interpolation near the Γ-point at large wave lengths will fail. In practice the fix is to use the Born effective charges calculated from density functional perturbation theory (DFPT) to construct a long-ranged dynamical matrix via Ewald techniques for the supercell in question and calculate the long-ranged real space FCs $\Phi_t ext LR$ due to the interacting Born-charges (dipoles). The short-ranged FCs Φ_{SR} are fitted to the remainder of the DFT forces

$$F_{\mathrm{DFT}} - (-\Phi_{LR} u) = -\Phi_{SR} u. \tag{3.13}$$

Now the FCs are separated in a long-ranged analytical part and a short-ranged fitted part and the analysis can continue as usual for any intermediate points.

3.2 Phonons

This section provides a short introduction to LD and the theory of phonons. For a more thorough overview see, e.g., [52] and the books listed in the beginning of this chapter.

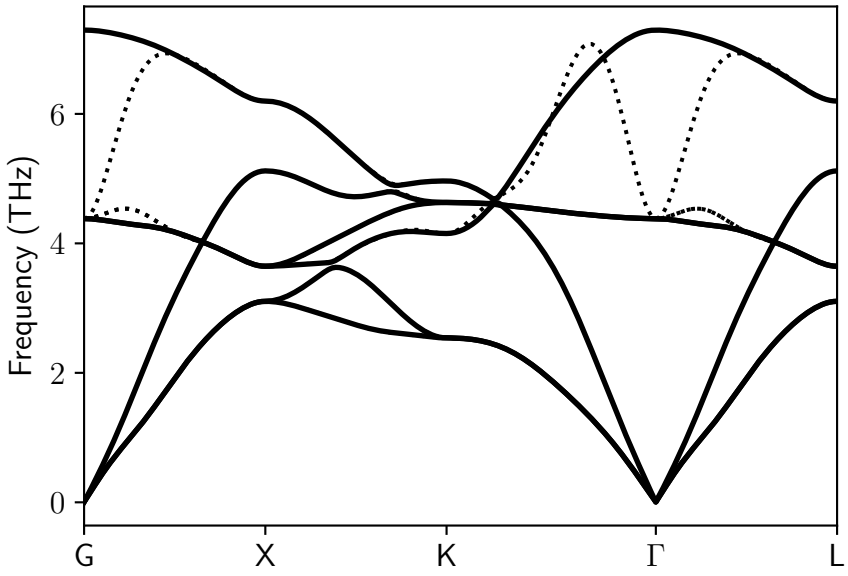

Figure 3.4: Dispersion relation of NaCl. The solid lines include the non-analytical correction (NAC) and the LO-TO splitting for $\boldsymbol{q} \to \Gamma$ is correctly reproduced. The dotted lines are without the NAC and thus no splitting is observed.

The basi(c)s for understanding the thermodynamics of vibrations in crystals is the phonon picture. In the harmonic approximation only the second-order FCs are kept and the Hamiltonian is exactly solvable. The solutions to this system in the framework of quantum mechanics are called phonons (in classical mechanics they are sometimes called normal modes). These solutions are typically regarded as quasi-particles but can be equally categorized as collective excitations. Nevertheless, the particle picture is especially useful in the context of the PBTE which we will come across later in Chapter 5. In addition, the exactly solvable model serves as a starting point for, e.g., mean field theories or Green's function methods to calculate higher-order corrections to physical observables due to the anharmonicity. The theory is covered in many text books and starts with the real space representation of the PES leading to the following Hamiltonian

$$H = \sum_{n\mu\alpha} \frac{\left|p^{\alpha}_{\mu}(n)\right|^2}{2m_{\mu}} + \frac{1}{2} \sum_{\substack{n,n' \\ \mu\nu \\ \alpha\beta}} \Phi^{\alpha\beta}_{\mu\nu}(n,n') u^{\alpha}_{\mu}(n) u^{\beta}_{\nu}(n'). \tag{3.14}$$

Via the dynamical matrix

$$D^{\alpha\beta}_{\mu\nu}(k) = \sum_n \frac{\Phi^{\alpha\beta}_{\mu\nu}(0,n)}{\sqrt{m_\mu m_\nu}} e^{-ik(R_\mu - R_\nu(n))} = \sum_s W^\alpha_{\mu s}(k)\omega^2_s(k)W^\beta_{\nu s}(k) \tag{3.15}$$

the new coordinates are in the form of lattice waves

$$q_s(k) = \sum_{\mu\alpha n} \sqrt{m_\mu} u^\alpha_\mu(n) W^\alpha_{\mu s}(k) \tag{3.16}$$

with polarization vectors W and frequencies ω. The Hamiltonian is thus diagonal and can be expressed in first quantization as

$$H = \frac{1}{2}\sum_{ks}\left(\left|p_s(k)\right|^2 + \omega^2_s(k)\left|q_s(k)\right|^2\right) \tag{3.17}$$

or in the framework of second quantization in terms of creation and annihilation operators

$$H = \sum_{ks}\left(\frac{1}{2} + a^\dagger_s(k)a_s(k)\right)\hbar\omega_s(k) \tag{3.18}$$

following standard procedures. From this we can exactly calculate thermodynamic properties of the crystal via, e.g., Helmholtz free energy F as

$$F = \sum_{ks}\left(\frac{1}{2}\hbar\omega_s(k) + \beta^{-1}\log\left(1 - \mathrm{e}^{-\hbar\beta\omega_s(k)}\right)\right). \tag{3.19}$$

From the above expressions it is apparent that the central objects of interest are the dispersion relation $\omega_s(k)$ and the corresponding polarization vectors $W^\alpha_{s\mu}(k)$.

3.2.1 Anharmonic phonons

The harmonic model of vibrations in crystals works very well in many cases,especially at low temperatures. However, with increasing temperature, anharmonic effects become important. Most notably, the harmonic model has infinite lifetimes and lacks thermal expansion. The phonons will move through the lattice without scattering and the standard PBTE breaks down. A first attempt to fix this is via the quasi-harmonic approximation where FCs are calculated at different volumes. From this information the volume dependence of the free energy can be calculated and related properties extracted such as Grüneisen and thermal expansion parameters.

The next step is to apply first-order perturbation theory with the third-order FCs as a perturbation. In this way the corrections to the energy levels of the phonons can be

determined and is to first order generally found to be imaginary with no shift in the frequencies. The lifetime is related to the imaginary part of the self energy

$$\tau_{\lambda}^{-1} = \frac{36\pi}{\hbar^2} \sum_{\lambda' \lambda''} \left|\Phi_{-\lambda\lambda'\lambda''}\right|^2 [\,(n_{\lambda'} + n_{\lambda''} + 1)\delta(\omega - \omega_{\lambda'} - \omega_{\lambda''}) + \\ (n_{\lambda'} - n_{\lambda''})(\delta(\omega + \omega_{\lambda'} - \omega_{\lambda''}) - \delta(\omega - \omega_{\lambda'} - \omega_{\lambda''}))\,],$$

where λ is a compound index over the momentum coordinate k and band index s. The lifetimes depend on the Fourier transformed third-order interactions and the temperature-dependent occupations n. This expression can be derived in a couple of ways see, e.g., [43, 53–55]. Since the interaction element contains crystal momentum-conserving delta functions the lifetimes depend not only on the strength of the interaction (anharmonicity) but also on the geometry of the dispersion relation. For example in BAs, which contains a large phonon band gap, higher order processes must be included to correctly describe the dynamics in the crystal[56] as the higher energy states (bands) cannot be reached from the low energy states via three-phonon processes due to energy (and momentum) conservation laws. This leads to the necessity to include fourth-order interactions in the thermal conductivity calculations motivating the efficient extraction of higher-order FCs. The need for higher-order FCs can also show up when when the harmonic phonons have negative energies (imaginary frequencies) as can happen in dynamically stabilized materials such as body-centered cubic (BCC)-Ti. If the harmonic phonons are still well behaved quasi-particles it is sometimes sufficient to calculate second-order corrections to the energies and lifetimes with ordinary perturbation theory. In second-order perturbation theory there is a contribution from both third and fourth-order FCs to both frequencies and lifetimes. Typically Green's function or variational methods are used to construct effective harmonic FCs corresponding to the renormalized propagators. For more information see, e.g., [57–59] and references therein.

4

Force constant extraction

As we saw in Chapter 3 the problem of extracting the free parameters for the FCs can be stated as a linear regression problem $Mx = F$ where the fit matrix is constructed from displacements in a set of supercells and the forces are obtained from, e.g., DFT calculations on the same supercells. In this chapter we will look at some methods to generate the displacements and to solve the linear regression problem using regularized regression methods.

In general, fitting a FC expansion (or any other type of interatomic potential) the method to fit the free parameters proceeds as follows and contains four important parts plus eventual feedback.

First an objective function (or loss function) must be defined. What do we want our potential to achieve? What properties are important to predict? Is it important to generalize? etc. Typical properties to include in the loss function are forces, energies, dimer energies, elastic constants, energies for different phases, or defect formation energies. For FCPs, however, they are due to their functional form quite limited to a specific lattice system and thus only forces (and sometimes energies) are typically included. In practice the loss function is almost always the squared error of the forces plus a penalty on the parameters.

Next a method to minimize the loss function must be chosen. The loss function need not be globally convex and thus the optimization procedure to find the global minimum can be hard. However, often a local minima is enough and for linear models there are a vast array of suitable methods that we will discuss below.

Next the training data must be generated. Here, there are essentially two classes. Either the data is generated from some source/distribution such as enumerated configurations, AIMD, or semi-random (see Sect. 4.1.2), or the data is generated from the present model itself. The latter is a form of active learning and the preferred method in most circumstances. It can also be thought of as a self-consistent effective model as

well, as discussed later.

Finally the model must be evaluated in order to combat overfitting by considering the effect of changing hyper-parameters on the predictions of unseen data. Therefore there exists a number of techniques for validation some of which will be briefly described.

4.1 Sampling of configurations

4.1.1 Systematic enumerations

Systematic enumeration is the most straightforward way to generate fit data. By displacing only one or a few atoms in a supercell the FCs can be read of directly from the forces or extracted via a simple least-squares fit. The procedure has been used extensively in the past with very good results for second order FCs in many systems. The procedure generates the exact amount of data needed in order to correctly identify all FCs and each configuration contains minimal noise. The procedure can in principle be used for higher order FCs as well but gets prohibitively expensive for disordered systems or high orders. Many software packages implement this method, which is often called the small displacement method introduced by Parlinski, Li, and Kawazoe [51]. Examples include PHONOPY[60] for second-order FCs and THIRDORDER.PY[61], PHONO3PY[53], and ALAMODE[54] for third-order FCs.

4.1.2 Rattle and Monte Carlo-rattle

The fundamental issue with the systematic enumeration is the low information content per configuration. This can be achieved by randomly displacing all the atoms and solving the corresponding regression problem that arises. This method is sometimes called the regression method and was introduced by Esfarjani and Stokes [46]. They also argued that the noise in the data is effectively canceled due to the random nature of the displacements adding to the benefits of the increased information content. Many methods exist for generating suitable configurations and the most simple one is the rattle method where a random displacement drawn from a normal distribution is applied to each atom individually. This can be seen as modeling the crystal as an Einstein crystal. It is a simple method but can lead to unphysical configurations probing unwanted anharmonicity in the crystal. The reason for this is that displacements for low temperatures are typically very correlated and heavier atoms typically move less. While it is possible to work around this problem using constrained rattle methods based on, e.g., Monte Carlo approaches it is often better to go directly to the phonon-rattle method.

4.1.3 Phonon-rattle

The problem with the previous approaches are the unphysical and uninformed sampling of the PES without any prior knowledge. Once an approximate harmonic model has been generated from some set of data a new set can be generated by populating the phonon modes of the current model at a low temperature. This can be accomplished by drawing phonon occupations from a normal distribution with variance

$$\sigma^2 = \frac{\hbar}{2\omega} \coth \beta\hbar\omega/2 \tag{4.1}$$

as described in [62]. In this way a bootstrap procedure is introduced where a new model is constructed based on the physically sound displacements of the previous model. Care must be taken so that the displacement are large enough (i.e., the temperature should not be too small) so the correct coefficients can be discerned from the noise in the DFT data but small enough so that we are still sampling the harmonic regime. Thus anharmonic terms are in general included in the expansion to mitigate the effect of anharmonicity when the goal is to recover the true harmonic FCs not only when using phonon-rattle. The phonon-rattle approach can be seen as the 0 K variant of the self consistent phonon method to be discussed later.

4.1.4 Variational principles

The choice of fitting the forces has an interesting relation to a variational principle via the Bogoliubov inequality. By applying Jensen's inequality ($\psi(\langle X \rangle) \leq \langle \psi(X) \rangle$ for ψ convex) to the Zwanzig free energy perturbation formula for the free energy F difference ΔF between two systems with Hamiltonians H and $\tilde{H}$

$$\Delta F = \tilde{F} - F = -\beta^{-1} \log \left\langle e^{-\beta \Delta E} \right\rangle_H = \langle \Delta E \rangle_H - \frac{\beta}{2} \left\langle \Delta E^2 \right\rangle_H \leq \langle \Delta E \rangle_H \,, \tag{4.2}$$

it is possible to establish a variational principle for the model (H) free energy F. In other words, the model free energy is minimized under the constraint that the first cumulant is zero. By applying this idea it is possible to show that using the ordinary least-squares loss function for the forces f on a harmonic model

$$\min \left\langle \left(f - \tilde{f} \right)^2 \right\rangle_H \quad \text{subject to} \quad \langle \Delta E \rangle_H = 0 \tag{4.3}$$

is equivalent to

$$\min F \quad \text{subject to} \quad \langle \Delta E \rangle_H = 0. \tag{4.4}$$

where the minimization is with respect to the free parameters of the model, i.e., the FCs. In the true ensemble the same holds but the model free energy must be maximized

instead. Notice that in practice the constraint is trivially enforced by the constant term in the model Hamiltonian.

This establishes a rationale for these methods and the above relations can also be obtained in the quantum case. Two common methods to be described below are based on this idea and differ whether the sampling is in the true ensemble or in the model ensemble.

4.1.5 Self-consistent harmonic phonons

If the procedure is based on sampling the same model we want to construct, it is called a self-consistent method [59]. In LD it is often called the self-consistent harmonic approximation (SCHA) or just the self consistent phonons (SCP) method and it is described in, e.g., [42]. These methods have firm roots in theoretical techniques such as Green's function methods and diagrammatic perturbation theory or the statistical perturbation method based on operator renormalization [63]. In practice on a computer we can generate displaced configurations and fit an harmonic model to the forces iteratively until the procedure has converged. The initial guess of the FCs is often in the form of an Einstein crystal and then as the model improves new configurations are generated using, e.g., the phonon rattle method. A variation of this method is the stochastic self-consistent harmonic approximation (SSCHA) where the free energy is minimized using a stochastic gradient descent method [63–67]. In practice this makes it easy to minimize also the Gibbs free energy by varying the cell metric. One of the main problems with any harmonic method is that it is only possible to effectively capture anharmonic effects in the harmonic FCs up to a certain degree. This can be partly remedied by including anharmonic effects in the sampling and in the model. The second large problem is deterioration of the ensemble average as the model improves. The old configurations are based on a different model than the present and thus all ensemble averages will be short-term biased. Clever methods exist, however, to discard configurations deemed to be of no use for the current model and thus the convergence can be sped up by including less data, a kind of bias-variance trade-off.

4.1.6 Effective harmonic models

An alternative is to sample configurations from AIMD simulations. This ensures physical configurations but can be expensive depending on the underlying ab initio method, code, system and so on. This method is sometimes called the temperature-dependent effective potential (TDEP) method after the eponymous program [68–70]. With this method effective harmonic models (EHMs) can be generated where higher-order FCs have been captured (or renormalized) into the second-order FCs. This allows for the calculation of temperature-dependent phonons and related quantities. Naturally also higher-order models can be constructed in this way to access, e.g., lifetimes [71]. The

main downside of this method is the expensive sampling, especially if quantum effects must be taken into account. This can be partly overcome by stochastic initialization and up-sampling techniques. Effective harmonic models can also be used to access otherwise hard to get properties via LD even when a cheap analytical potential is used where properties are (in principle) accessible using other methods. In this fashion it is, for example, possible to calculate free energies via an EHM instead of via thermodynamic integration.

4.1.7 Anharmonic higher order models

Lastly there is the possibility to construct effective or self-consistent anharmonic FC models. With this method anharmonic expansions are fitted to either AIMD or the model itself is sampled using MC or MD. While MD has been performed using FCs [72], to the best of my knowledge self-consistent anharmonic models were not done before Brorsson *et al.* [73]. In the limit of infinite order and cutoff this method should produce the same true expansion of the potential energy surface independent of whether the sampling is in the true or model Hamiltonian. In practice this method using anharmonic FCs and MD allows for non-perturbative treatment of high-order perturbations, e.g., up to fourth order in the energy expansion. This can be useful where normal perturbation theory struggles. In addition the self-consistent procedure ensures that the PES is stable for reasonable configurations. Typically an anharmonic FCP will be somewhat unstable when running MD if the training data is not diverse enough. This can often be fixed by including configurations from an MD run close to where the system misbehaves. Unfortunately many systems exhibit natural defects which can be created spontaneously in MD simulation when the PES is soft, e.g., close to melting [35]. In theses situations FCPs are ill suited although there have been attempts to artificially stabilize/constrain the expansion. The problem with anharmonic FCPs in general is that even if a good model is found it is not necessarily easier to find accurate properties of interest from this model compared to a lower order model. For example, the free energy via perturbation theory from a self-consistent fourth-order model might not be more accurate than the exact free energy from a self-consistent harmonic model due to the extra level of approximations when dealing with fourth-order FCs.

4.2 Regularized Linear Regression

Once structures are generated the FC expansion can be constructed using linear regression as long as the corresponding properties are linear functions of the free parameters (e.g., forces and energies). When there is plenty of training data, and the data is homogeneous there is often no reason not to use OLS. In Fig. 4.1 a typical learning curve is shown. For low amount of data the training error is very different from the

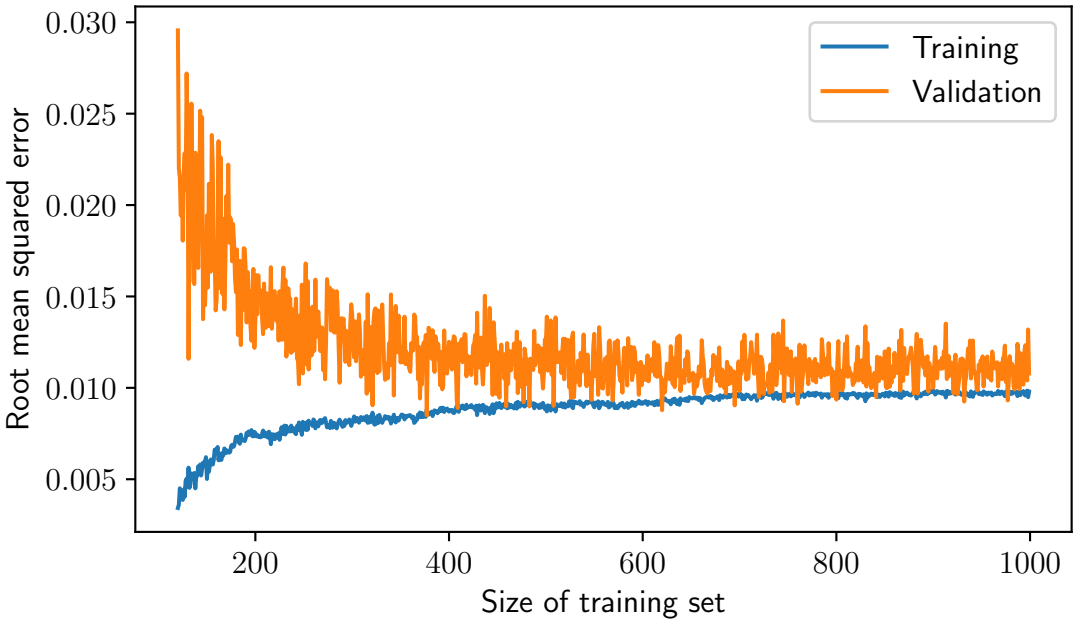

Figure 4.1: Typical learning curve. As the training set increases the training error goes up (less overfitting) while the validation error goes down until they meet at the noise level.

validation error indicating overfitting. However, even when the resulting fit matrix is larger than the number of parameters, the matrix rank can still be lower and thus the regression problem can still be ill-conditioned. This can, for example, happen in systems with a large primitive cell. Regularized regression is a technique used to combat over-fitting and used together with cross-validation to assess the performance of the resulting model, see [74–76] for applications to FCs where it is sometimes called compressive sensing (CS).

During regularized linear regression in addition to the (typically) squared error imposed on the difference in forces an extra term is introduced to penalize large parameter vectors. Thus not only must we find an accurate model but we must find it using few or small parameters. Two common approaches are least absolute shrinkage and selection operator (LASSO) (L_1) and ridge regression (L_2) which are typically defined as

$$\min_x \|Ax - b\|_2 + \lambda \|p\|_n \tag{4.5}$$

where the choice $n = 1$ is called LASSO and $n = 2$ is called ridge regression. The parameter λ is called the regularization parameter and controls the trade-off between bias and variance errors. A high bias error means that the model is unable to predict patterns in the data and is thus under-fitted. If the variance error is high the model is sensitive to noise in the training data and is over-fitted.

Many regularization techniques can also be formulated in a Bayesian framework. The LASSO method is for example equivalent to a Laplace prior distribution together with an assumption of Gaussian noise. The reformulation of the regularization problem in terms of Bayesian inference provides powerful tools to quantify uncertainties in the models. It is, for example, possible to assess the effect of uncertainties in the PES on the dispersion relation and use such error estimation to steer model construction.

4.2.1 Feature selection

A natural consequence of the regularization is that we get information about what features in our model matter and which do not. Feature selection (and regularization in general) has different names in different fields. In signal processing it is called compressed sensing and is typically based on l_1 regularization, i.e., LASSO. By assuming sparse solutions of the problem the set of possible solutions can be reduced and consequently signals can be recovered even when the amount of data is seemingly not enough. From a Bayesian point of view we can regard it as a prior knowledge about the correlation between the solution coefficients where we encode that not all coefficients can be large at the same time.

Popular methods include recursive feature elimination (RFE) and orthogonal matching pursuit (OMP) which can be added on top of any standard training method. In RFE the least important features are dropped iteratively starting from a full solution. In OMP features are instead iteratively added from a zero solution. Bayesian methods include automatic relevance determination regression (ARDR) which puts individual Gaussian priors on the coefficients and eliminates coefficients if their magnitude relative to the posterior falls below a pre-defined threshold.[1]

All methods discussed have one or more hyper-parameters that must be tuned. They can either be the number of features or some continuous parameter(s). In either case cross-validation can be used to determine optimal hyper-parameter to use.

4.2.2 Cross validation

In order to assess the performance of the model and to mitigate both over and underfitting cross-validation should be performed. The generated data is divided in three sets: training, validation, and testing. Typically the training set is large compare to the two other sets. The training set is used to fit the model and the validation set is used to optimize the regularization parameter. If a large amount of data is available the training error and the validation errors are the same, see Fig. 4.1. This is equivalent to saying that the learning curve has converged. If the validation error is at a minimum with respect to the regularization parameter but much larger than the training error

[1]The threshold value is a hyper-parameter of this method.

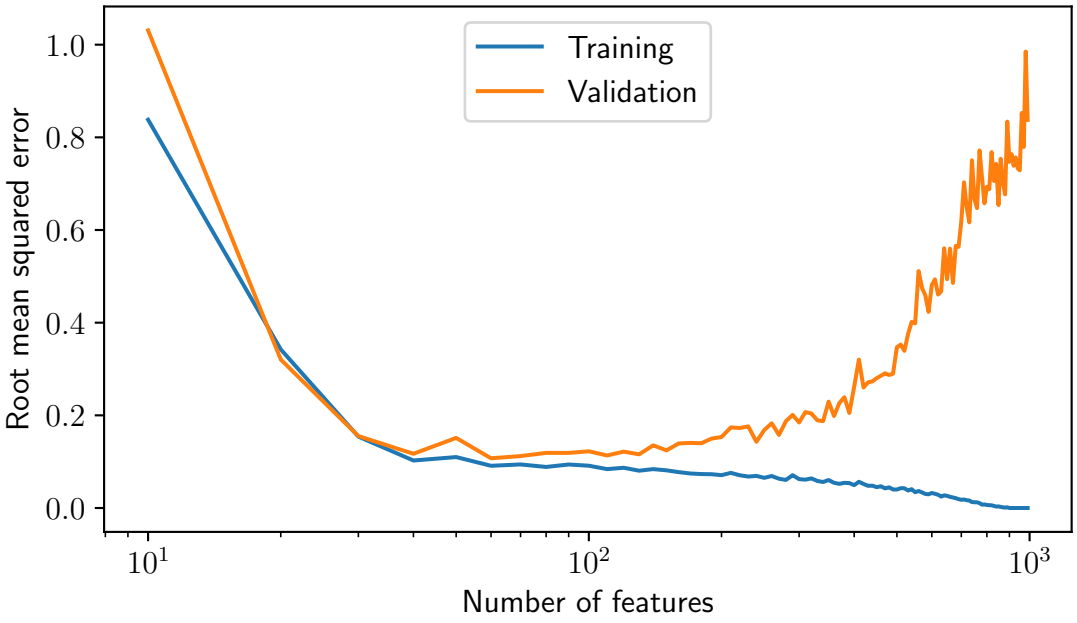

Figure 4.2: Typical hyper-parameter scan with RFE. The training error decreases monotonically as the model increases in complexity. At a certain point the validation error goes up indicating overfitting. The minimum of the validation curve should in principle correspond to the best generalization but in practice less complex models (less features) may be preferred.

we are in principle over-fitted but the error stems from lack of data, see Fig. 4.2 for an illustration. Once the optimal hyper-parameters have been selected the final model can be evaluated again against the test set. If the scores on the validation and test sets are similar the optimal choice of hyper-parameters should be independent of the choice of validation set.

In addition to the root mean squared error (RMSE) information criteria can be used, such as Akaike information criterion (AIC) and Bayesian information criterion (BIC). For Gaussian errors the BIC is given by (lower is better)

$$\mathrm{BIC}(k|n) = n \log(\mathrm{MSE}) + k \log(n), \tag{4.6}$$

where n is the number of samples and k the number of parameters. Here, we can see that the BIC balances low error (low mean squared error (MSE)) against a complex model (large k). Such criteria can aid in automatic determination of optimal models.

5

Thermal transport

There are many approaches for calculating the thermal conductivity in condensed matter systems. Loosely they belong in three classes based on thermostats, fluctuations via the GK relations, and PBTE[77], respectively.

The most straightforward approach is non-equilibrium molecular dynamics (NEMD) where two separated regions in a MD simulation are held at different temperatures using thermostats. The heat will flow from the hot region to the cold via an intermediate region, which evolves under NVE conditions. The thermal conductivity can simply be calculated from the temperature gradient and the amount of heat that is pumped between two thermostated regions per unit time. This is a conceptually simple method and very useful for measuring interface conductivities. For bulk conductivities, however, the method has some drawbacks. First, the temperature gradient is typically very large as the temperature difference needs to be larger than typical fluctuations while the length scales are typically quite short. Second, the spatial limitation, or boundary conditions, in the simulation may impose an artificial wavelength/mean-free-path cutoff similar to a boundary scattering term in PBTE [53, 78]. Since the low lying acoustic modes, which have typically long mean free paths, carry much of the heat this can lead to an underestimation of the lattice thermal conductivity (LTC). Fortunately, as the temperature increases the mean free path decreases so this is typically more problematic for low temperatures where other approaches (PBTE) can be taken instead.

The two other methods will be discussed in this chapter in some detail starting with the PBTE.

5.1 Peierls-Boltzmann transport equation

When the motion of atoms in a solid is highly correlated it is often useful to make a Fourier transform and instead describe the motion in terms of the resulting collective

excitations (phonons) as described earlier in Chapter 3. The resulting phase space is now given by the phonon coordinates and momenta, and the quasi-particles are effectively assumed to behave similarly to the particles in a dilute gas. This system is called a weakly interacting Bose gas as the phonons follows the Bose-Einstein statistic. Here the heat carriers are the phonon quasi-particles and the corresponding PBTE is solved by constructing a scattering integral based on the phonon-phonon interactions calculated from anharmonic FCs using, e.g., Green's function methods as described in Chapter 3. The method thus relies on an accurate description of the PES in terms of FCs. Although the method contains a semi-classical leap of faith the possibility of including quantum effects via the populations is very attractive. For many materials 0 K or effective third-order FCs are enough but for some materials 4-phonon interactions are important and thus the corresponding rates must be included [56, 79]. The main issue with PBTE is the computational cost of constructing FCs and solving the PBTE for systems with large primitive cells, e.g., systems with complex crystal structures or disordered systems.

However, in order to relate the motion of the phonons with macroscopic transport we need to have some kind of notion of localization. While formally the phonons are only exact excitations for an infinite/periodic crystal and thus spread out over a large region they can be localized in space by considering wave packets. The physical picture is thus that phonons are created at a certain macroscopic point in space and travel for a time as a wave packet and are annihilated at another point in space later, resulting in the transfer of energy and heat. Theses wave packets thus have a frequency ω, a speed of propagation $v = \partial_q \omega$ and a lifetime τ. In addition we can think of each wave packet carrying some energy $\hbar\omega$ and thus a wave packet that is created (excited) at a point x in the system will carry an energy $\hbar\omega$ with speed v for a time τ before being annihilated at a point $x' = x + v\tau = x + \Lambda$ where Λ is the mean free path. The reason why there is a flow of heat is because of the difference in phonon populations at different points in space due to the thermal gradient. It is this difference in populations we calculate using the PBTE. Now the formalism will be briefly described. For a more extensive account of PBTE see, e.g., [40, 80] and for ab initio thermal transport in general see [81].

The Peierls-Boltzmann theory of thermal transport begins with the assumption of a well defined local equilibrium distribution function

$$n^0_\lambda(T(x)) = \frac{1}{e^{\hbar\omega_\lambda / k_B T(x)} - 1} \tag{5.1}$$

for the mode λ which is defined by the lattice momentum and band index. The spatial variation enters through the spatial variation of the temperature. The phonon transport equation is now equivalent to the transport in the kinetic theory of gases. First the Liouville equation is integrated down to a single particle distribution function to yield

the Boltzmann equation

$$\frac{\mathrm{d}\rho}{\mathrm{d}t} = 0 \quad \Longrightarrow \quad \frac{\mathrm{d}n_\lambda}{\mathrm{d}t} = S(n) \tag{5.2}$$

with the assumption that the scattering integral S depends only on the single particle distribution itself. In more detail we have

$$\frac{\partial n_\lambda}{\partial t} + \frac{\partial n_\lambda}{\partial x} v_\lambda = S(n). \tag{5.3}$$

In equilibrium with no spatial temperature gradients this turns into

$$\frac{\partial n^0_\lambda}{\partial t} = S(n^0). \tag{5.4}$$

If we assume that the change in occupation due to the thermal gradient is a small perturbation to the equilibrium distribution $n = n^0 + n'$ we arrive at

$$\frac{\partial n'_\lambda}{\partial t} + \frac{\partial n^0_\lambda}{\partial T}\frac{\partial T}{\partial x} v_\lambda = S(n) - S(n^0) \tag{5.5}$$

after the assumption that the gradient of n' with respect to T is small. If we assume the temperature gradient to vanish, we see that the scattering integral brings the out-of-equilibrium occupation back to the equilibrium one, at which point we introduce the relaxation time approximation (RTA) which states that the backwards transition is proportional to the perturbation. The lifetime can be taken to be the inverse of the self energy of each phonon as described earlier and will depend on the occupations via the scattering rates. In the steady state regime ($\partial_t n' = 0$) the linearized PBTE within the RTA reads

$$\frac{C_\lambda}{\hbar\omega_\lambda} \nabla T v_\lambda = -\frac{n'_\lambda}{\tau_\lambda(n)} \tag{5.6}$$

with the heat capacity $C = \hbar\omega\partial_T n^0$. Here, we see a problem as the lifetime depends on the unknown perturbation. In the single-mode relaxation time approximation (SMRTA) we simply set the lifetime to be that of the unperturbed system, in which case the change in occupations can be written as

$$n'_\lambda = -\tau_\lambda(n^0)\frac{C_\lambda}{\hbar\omega_\lambda} \nabla T v_\lambda. \tag{5.7}$$

This equation makes sense as the negative occupation means less phonons are going in the positive direction towards higher temperatures.

The above equation can also be exactly solved via iterative approaches where the occupations are reinserted to calculate the new lifetimes or via direct inversion. The

main drawback of the SMRTA is that it underestimates the so called repopulation of modes which is important for some materials [82]. It is also possible to include higher-order processes when calculating the relaxation times as described in Chapter 3 and as implemented in [79].

For the final expression the heat current is defined by the formula

$$J = -\frac{1}{V}\sum_{\lambda} \hbar\omega_{\lambda} n'_{\lambda} v_{\lambda} \tag{5.8}$$

which is basically multiplying the energy per mode, the number difference of phonons in the mode, and the velocity of the mode. With the above expression for the perturbation the thermal conductivity coefficient is

$$\kappa = \frac{1}{V}\sum_{\lambda} C_{\lambda} v_{\lambda} \Lambda_{\lambda} \tag{5.9}$$

where $\Lambda = v_{\lambda}\tau_{\lambda}$ is the mean free path and C is the heat capacity of the mode.

Novel insights into PBTE include the Wigner formulation described in [83, 84] where glass-like transport is more readily handled. The method is implemented in both PHONO3PY and KALDO[85].

5.2 Green-Kubo thermal transport

For an excellent overview of the GK formalism see [86] which is the basis for this short introduction. In the 1950s Green and Kubo developed a theory of linear transport based on the work of Callen and Welton on the fluctuation-dissipation theorem. The theory relates equilibrium fluctuations expressed as time correlation functions with the corresponding transport coefficients.

$$\kappa \propto \int_0^{\infty} \langle J(t)J(0)\rangle \, \mathrm{d}t \tag{5.10}$$

Thus a MD simulation can be performed in the NVE ensemble and the auto-correlation of the heat flux J is measured to provide the thermal conductivity coefficient κ. This equilibrium molecular dynamics (EMD) approach is thus a very general method and in principle free from bias as the system evolves without any external perturbation.

Compared to the NEMD method the effect of boundary conditions is not as severe. Although the allowed wave vectors are limited their mean free paths are not as the the modes are free to propagate through the periodic boundary conditions. The main problem lies in the challenge to adequately sample the correlation function, especially for harmonic materials with long life times (i.e., materials with a large LTC). This can be overcome by the use of clever methods from signal analysis allowing even the direct use of AIMD, see again [86].

5.2.1 Local energy and the continuity equation

For a macroscopic system we stipulate that there exists a energy density function $e(x, \Gamma)$ that measures the local energy at a point x in the system in state Γ. This density is related to the total energy of the system via

$$\int e(x, \Gamma) \mathrm{d}x = H(\Gamma), \tag{5.11}$$

where Γ is a point in the phase space of the system and $\mathrm{d}x$ is large compared to the range of the interatomic interactions. The energy is furthermore a (locally) conserved quantity and thus the energy density obeys the continuity equation

$$-i\omega e(q, \omega) = -iqj(q, \omega) \tag{5.12}$$

for some heat current density j. The long-wavelength parts of conserved densities are called hydrodynamic variables and our goal now is to find their equations of motion.

5.2.2 Linear constitutive equations

In the small field limit the equation of motion for the energy density can be linearized in Fourier space

$$-i\omega e(q, \omega) = \Lambda(q, \omega) e(q, \omega) \tag{5.13}$$

and we can thus identify the heat current density as

$$j(q, \omega) = \frac{1}{-iq} \Lambda(q, \omega) e(q, \omega). \tag{5.14}$$

From general considerations the constant and linear term must vanish in Λ due to causality and parity considerations. As such, the macroscopic flux $\boldsymbol{J} = \int j \, \mathrm{d}x$ and the macroscopic density gradient $\boldsymbol{D} = \int \nabla e \, \mathrm{d}x$ are linearly related via $\boldsymbol{J} = \lambda \boldsymbol{D}$. Because of assumptions of local equilibrium of the state variables we can also write the relation in terms of the thermodynamic force $F = \int \nabla \beta \, \mathrm{d}x$ where $\beta = 1/T$ is the intensive conjugate variable to the internal energy and we arrive at

$$\boldsymbol{J} = L F \tag{5.15}$$

for some parameter L and force F to be determined. Note here that the natural cause of a heat current is actually the gradient of the inverse temperature. Nevertheless, in the linear regime any equivalent measure can be used and the corresponding transport coefficient will only differ by a function of the equilibrium state variables.

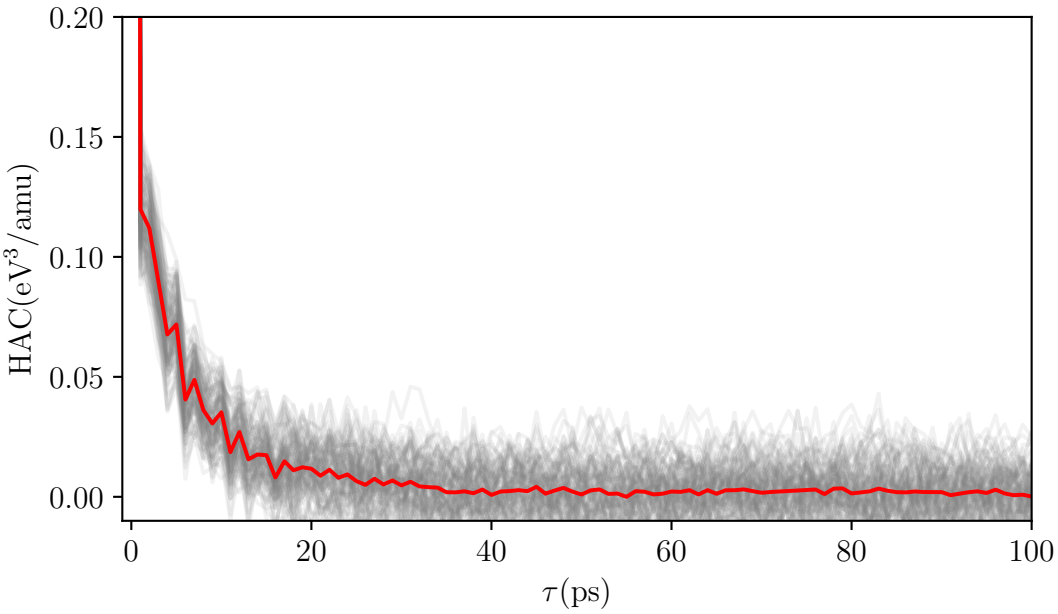

Figure 5.1: Heat current auto correlation (HAC) in the through plane direction of Graphite at 600 K. The gray curves are 100 individual simulations overlayed and the red curve is the unfiltered mean. At around 40 ps the correlation is almost zero and should be enough to get a converged value of the thermal conductivity.

5.2.3 Linear response

The GK relations allow us to calculate the parameter L by studying the equilibrium fluctuations of the flux J. Specifically for a perturbation $V = \int v(x)e(x)\,\mathrm{d}x$ with some coupling constant v (the driving field) to the original Hamiltonian the corresponding thermodynamic force is given by

$$F = \beta_0 \int \nabla v \tag{5.16}$$

and the corresponding transport coefficient is

$$L = \int_0^\infty \langle J(t)J(0)\rangle_0 \,\mathrm{d}t. \tag{5.17}$$

For a coupling field $v = -\Delta T/T_0$ the (mechanical) perturbation mimics the effect of a temperature field. This will be important later for the homogeneous non-equilibrium molecular dynamics (HNEMD) method where this observation allows us to study the heat current response to a perturbation. Continuing, the corresponding force for the

above perturbation just becomes the temperature (T) gradient and the final value for the thermal conductivity is given by

$$\kappa = \frac{1}{V k_B T^2} \int_0^\infty \langle \boldsymbol{J}(t)\boldsymbol{J}(0)\rangle_0 \, \mathrm{d}t. \tag{5.18}$$

Now the only thing left is a local definition of heat or internal energy that is consistent and compatible with both our microscopic and macroscopic understanding. This can be conceptually challenging due to the ambiguity in the localization of the internal energy. Recent research has, however, shown that the exact definition of the energy density on the atomic level is not important [86]. As long as general principles are obeyed all definitions should give equivalent results. Thus from the conservation of energy and from the local character of the interatomic potential we stipulate that in the thermodynamic limit of coarse graining there must exist a local measure of the internal energy obeying the continuity equation for a suitable definition if the heat flux. In practice the energy is divided up into atomic energies

$$E = \sum_i E_i = \sum_i \frac{p_i^2}{2m_i} + V_i(x) \tag{5.19}$$

and each atom is considered a heat carrier and the corresponding current is analogous to, e.g., a mass or charge current.

5.2.4 Homogeneous non-equilibrium molecular dynamics

The EMD method can also be combined with a perturbing thermostat in order to artificially increase the fluctuations and thus provide a stronger signal to noise ration, leading to faster computational convergence. Evans *et al.* [87] showed that a time-dependent field $F(t)$ could be used to drive the system out of equilibrium, enhancing the fluctuations. By studying the correlation between the driving force and the response of the heat current the thermal transport coefficient can be calculated using a simple formula relating the force to the induced heat current

$$\frac{\langle \boldsymbol{J}(t)\rangle}{TV} = \kappa F(t). \tag{5.20}$$

Fan *et al.* generalized this method to many-body potentials [88] and implemented it specifically for HNEMD [89] in the GPUMD software package used in Paper III.

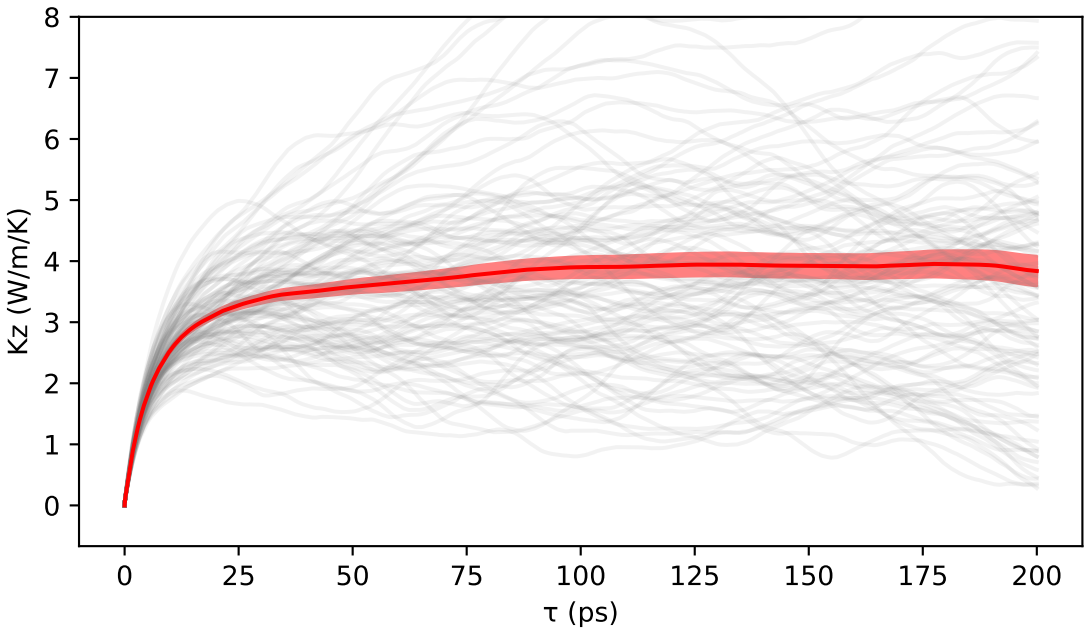

Figure 5.2: Running thermal conductivity corresponding to Fig. 5.1. The gray lines show the results from 100 individual simulations while the red curve shows the mean and standard deviation. After around 40 ps the thermal conductivity is converged within the specified error.

6

Summary of papers

Paper I

The Hiphive Package for the Extraction of High-Order Force Constants by Machine Learning.

Paper I is the first of a set of papers related to the extraction and application of FC expansions. In this paper we present methods and workflows as well as some demonstrations of the HIPHIVE package that we developed. The focus is on the advantages of an easy framework to work with FCs and how to use auxiliary software such as SCIKIT-LEARN to accelerate the regression extraction. The main features of HIPHIVE are presented as well as the concepts necessary to work with FCs in practice. We successfully implemented proper handling of both local crystal symmetries as well as global symmetries such as translational and rotational invariance. HIPHIVE handles FC expansions up to arbitrary order allowing for accurate descriptions of complex PESs. This allows, for example, exact non-perturbative treatments of properties of interest. The translational symmetries are exactly fulfilled by using integer numerics to find the kernel of the translational sum rule constraint matrix. Demonstrations include proper handling of rotational invariance and phonon dispersions of the two-dimensional material MoS_2 as well as the thermal conductivity. Furthermore we demonstrate how to use higher-order FCPs to run MD via the ASE library.

Paper II

Efficient construction of linear models in materials modeling and applications to force constant expansions.

In paper II we used HIPHIVE in conjunction with SCIKIT-LEARN to benchmark and test the use of compressive sensing and related techniques to the FC extraction problem in the setting of the regression approach. The regression method can vastly cut down the number of DFT calculations needed and we tested several different methods including LASSO, adaptive LASSO, RFE, and ARDR on different systems. In terms of methods RFE with OLS works well in many cases while ARDR tend to suffer from bad scaling as the training size increase.

The single most important thing when fitting FCs is to tune the cutoffs properly. While the regularized regression methods should in principle be able to find the correct parameters and discard clusters that are outside the interaction length of the potential the size of the training size might be too large to handle for some algorithms.

The second important observation is that for some physical properties the accuracy does not scale with the RMSE measure. This highlights the pitfalls of blindly optimizing for this measure and led us to conjure that using estimators from information theory such as BIC and AIC should provide more sensible models. Furthermore the highly popular LASSO method does not perform as well as some other methods and suffers from over-selection. Therefore post-LASSO methods should be preferred such as adaptive-LASSO. Finally we demonstrated that temperature-dependent thermal conductivities including fourth-order effective renormalization and beyond is computationally feasible.

In conclusion, despite CS being somewhat useful for configurational cluster expansions [90, 91], we did not find the methods very useful for our systems compared to Zhou *et al.* [92]. For FC expansions it is much easier to generate new data as each configuration contributes $3N$ new data points for systems where the cutoffs are comparable or longer than the size of the system. We also found that a naïve use of advanced regularized regression methods can sometimes add a significant cost so care must be taken.

Paper III

Extremely anisotropic van der Waals thermal conductors.

In paper III we tried to confirm and explain the extremely low through-plane conductivity of rotationally disordered MoS_2 van-der-Waals structures. The work was a collaboration with the groups of David Muller, David Cahill, and Jiwoong Park who performed the synthesis and experimental measurements. The main challenge was the complexity of the unit cell for these kind of materials. Molybdenum disulfide MoS_2 consists of stacked layers of single sheets much like graphite is build from stacked layers of graphene. These types of materials have been studied before [93] in the bulk config-

uration with small unit cells using PBTE and the transport mechanism is rather well understood. For rotational disorder, however, things become complicated as the size of the cell grows rapidly at low inter-planar angles. While many studies has been done on so-called Moiré structures where for some magic angles two layers rotated relative to each other can fit in the same supercell the studies have been mostly on bilayers. It is also computationally prohibitive to use PBTE directly on such systems as the primitive cell is very large.

Thus we came up with an algorithm to stack many layers on top of each other with random interlayer rotations while allowing for some strain in each layer. To calculate the thermal conductivity we used the HNEMD method [87] together with an analytical potential [94] implemented in GPUMD [95]. Using this approach we could replicate nearly quantitatively the experimental measurements, most crucially the drop in the through-plane conductivity confirming the claim of an extremely high anisotropy in the thermal conductivity. We speculate that the microscopic mechanism can be related to the extreme softening of the through-plane transverse modes. However, it might also be due to general disorder arguments as the coupling between longitudinal through-plane and in-plane modes increases.

7

Outlook

The maturity of the present array of software and methods made available during the last decades opens up many possibilities: From a practical point we want accurate methods that can predict properties with low computational cost and limited human input. This is the goal of so-called high-throughput studies [96] but unfortunately this is hard to pull of in practice as there are as many details as there are materials. Another angle is to make certain types of standard procedures semi-automatic for the end user. One such attempt is active learning of ML potentials which has been successfully applied to a range of systems, see, e.g., [97, 98]. A third approach is to sacrifice computational cost for human cost and go directly from ab initio calculations to properties of interest via exact methods such as Green-Kubo [99, 100]. Of course this is kind of kicking the can down the road you can argue as there are approximations made even in DFT, nevertheless this type of methods will probably grow in popularity.

As methods become more and more precise the question of accuracy becomes more important. At one point the errors made in certain approximations such as, e.g., the PBTE will be smaller than the errors in input data obtained from ab initio techniques. In addition many properties of condensed matter systems are ignored such as interactions of phonons with other excitations and DOFs such as electrons and spins as well as structural properties such as defects and boundaries.

For the construction of FCs some questions are still open (at least from my perspective) concerning the relationship between different methods. For example, when should EHMs be preferred over SCP? What is actually being optimized in the different self consistent procedures? How are the derived properties related to the observed properties? One interesting idea is to compare PBTE and GK directly by using a FCP directly as input. The details of recent progress of relating PBTE and GK can thus be explored in practice on the same footing.

In terms of future development of HIPHIVE there is still missing the ability to handle

cell deformations. This can also naturally be related to FC expansions in internal coordinates similar to classical intra-molecular force fields used in chemistry. This would also be a natural framework to start for studying disordered systems. Of course there is always a point for any basis when its efficacy breaks down and with the increased popularity of ML potentials many properties could perhaps more easily be obtained by constructing a suitable ML potential. However, at the end we wish to learn something about the underlying physics and thus there will remain a need for simpler potentials. Just as ML potentials bridge analytical potentials and ab initio methods, maybe there is something between a deep NN and an analytical potential? After all it is the intermittent models that define the framework and language we use to explain physical phenomena.

Many of the above points culminate in the study of thermal conductivity in disordered vdW structures that continues beyond the third paper in this thesis. The nature of the thermal transport in these types of materials is still not completely understood. This despite there being accurate potentials providing the correct numbers.

Acknowledgments

Firstly, thank *you* for reading this far! Especially Adam for making it through my incoherent ramblings.

Next, a big thank to past and present members of the Materials and Surface Theory division and the Condensed Matter and Materials Theory division for making the office a great environment. Extra thank to my office mate Movaffaq and my co-supervisor Andreas!

Thank you Erik for making the development of HIPHIVE possible, standing ground against type hinting and being a great friend in general!

Thanks to my friends, past and present, and to my family for your support. I love you very much.

Finally, I can't thank my examiner Göran and my supervisor Paul enough for their support over the years despite testing their patience. Hopefully the coming two years will be more productive than the last two.

Bibliography

[1] C. R. Harris, K. J. Millman, S. J. van der Walt, R. Gommers, P. Virtanen, D. Cournapeau, E. Wieser, J. Taylor, S. Berg, N. J. Smith, R. Kern, M. Picus, S. Hoyer, M. H. van Kerkwijk, M. Brett, A. Haldane, J. F. del Río, M. Wiebe, P. Peterson, P. Gérard-Marchant, K. Sheppard, T. Reddy, W. Weckesser, H. Abbasi, C. Gohlke, and T. E. Oliphant, *Array programming with NumPy,* Nature **585**, 357 (2020). doi:10.1038/s41586-020-2649-2.

[2] A. H. Larsen, J. J. Mortensen, J. Blomqvist, I. E. Castelli, R. Christensen, M. Dułak, J. Friis, M. N. Groves, B. Hammer, C. Hargus, E. D. Hermes, P. C. Jennings, P. B. Jensen, J. Kermode, J. R. Kitchin, E. L. Kolsbjerg, J. Kubal, K. Kaasbjerg, S. Lysgaard, J. B. Maronsson, T. Maxson, T. Olsen, L. Pastewka, A. Peterson, C. Rostgaard, J. Schiøtz, O. Schütt, M. Strange, K. S. Thygesen, T. Vegge, L. Vilhelmsen, M. Walter, Z. Zeng, and K. W. Jacobsen, *The atomic simulation environment—a Python library for working with atoms,* Journal of Physics: Condensed Matter **29**, 273002 (2017). doi:10.1088/1361-648X/aa680e.

[3] N. Wirth, *A Plea for Lean Software,* Computer **28**, 64 (1995). doi:10.1109/2.348001.

[4] L. Verlet, *Computer "Experiments" on Classical Fluids. I. Thermodynamical Properties of Lennard-Jones Molecules,* Phys. Rev. **159**, 98 (1967). doi:10.1103/PhysRev.159.98.

[5] P. Hohenberg and W. Kohn, *Inhomogeneous Electron Gas,* Phys. Rev. **136**, B864 (1964). doi:10.1103/PhysRev.136.B864.

[6] W. Kohn and L. J. Sham, *Self-Consistent Equations Including Exchange and Correlation Effects,* Phys. Rev. **140**, A1133 (1965). doi:10.1103/PhysRev.140.A1133.

[7] N. Metropolis, A. W. Rosenbluth, M. N. Rosenbluth, A. H. Teller, and E. Teller, *Equation of State Calculations by Fast Computing Machines,* The Journal of Chemical Physics **21**, 1087 (1953). doi:10.1063/1.1699114.

[8] W. K. Hastings, *Monte Carlo sampling methods using Markov chains and their applications,* Biometrika **57**, 97 (1970). doi:10.1093/biomet/57.1.97.

[9] E. Fermi, J. Pasta, and S. Ulam, *Studies of nonlinear problems. I.,* Tech. Rep. LA-1940, Los Alamos, 1955.

[10] T. Dauxois, *Fermi, Pasta, Ulam, and a mysterious lady,* Physics Today **61**, 55 (2008). doi:10.1063/1.2835154.

[11] S. Nordholm, J. Forsman, C. Woodward, B. Freasier, and Z. Abbas, *Generalized van der Waals Theory of Molecular Fluids in Bulk and at Surfaces* (Elsevier, 2018). doi:10.1016/C2015-0-06831-9.

[12] M. S. Daw and M. I. Baskes, *Embedded-atom method: Derivation and application to impurities, surfaces, and other defects in metals,* Phys. Rev. B **29**, 6443 (1984). doi:10.1103/PhysRevB.29.6443.

[13] G. C. Abell, *Empirical chemical pseudopotential theory of molecular and metallic bonding,* Physical Review B **31**, 6184 (1985). doi:10.1103/PhysRevB.31.6184.

[14] J. Tersoff, *New empirical approach for the structure and energy of covalent systems,* Phys. Rev. B **37**, 6991 (1988). doi:10.1103/PhysRevB.37.6991.

[15] A. Stukowski, E. Fransson, M. Mock, and P. Erhart, *Atomicrex–a general purpose tool for the construction of atomic interaction models,* Modelling and Simulation in Materials Science and Engineering **25**, 055003 (2017). doi:10.1088/1361-651x/aa6ecf.

[16] M. P. Allen and D. J. Tildesley, *Computer Simulation of Liquids* (Oxford: Oxford University Press, 1987).

[17] M. Petisme, *Atomistic modeling of interfaces in WC-Co cemented carbides.* PhD thesis, Chalmers university of technology, 2015.

[18] J. Behler, *Perspective: Machine learning potentials for atomistic simulations,* The Journal of Chemical Physics **145**, 170901 (2016). doi:10.1063/1.4966192.

[19] J. Behler and M. Parrinello, *Generalized Neural-Network Representation of High-Dimensional Potential-Energy Surfaces,* Phys. Rev. Lett. **98**, 146401 (2007).

[20] J. Behler, *Four Generations of High-Dimensional Neural Network Potentials,* Chemical Reviews **121**, 10037 (2021). PMID: 33779150. doi:10.1021/acs.chemrev.0c00868.

[21] E. Kocer, T. W. Ko, and J. Behler, *Neural Network Potentials: A Concise Overview of Methods,* Annual Review of Physical Chemistry **73**, 163 (2022). PMID: 34982580. doi:10.1146/annurev-physchem-082720-034254.

[22] A. P. Bartók, M. C. Payne, R. Kondor, and G. Csányi, *Gaussian Approximation Potentials: The Accuracy of Quantum Mechanics, without the Electrons,* Phys. Rev. Lett. **104**, 136403 (2010).

[23] S. Chmiela, H. E. Sauceda, K.-R. Müller, and A. Tkatchenko, *Towards exact molecular dynamics simulations with machine-learned force fields,* Nature Communications **9**, 3887 (2018). Bandiera_abtest: a Cc_license_type: cc_by Cg_type: Nature Research Journals Number: 1 Primary_atype: Research Publisher: Nature Publishing Group Subject_term: Atomic and molecular physics;Chemical physics;Theoretical chemistry Subject_term_id: atomic-and-molecular-physics;chemical-physics;theoretical-chemistry. doi:10.1038/s41467-018-06169-2.

[24] L. Himanen, M. O. Jäger, E. V. Morooka, F. Federici Canova, Y. S. Ranawat, D. Z. Gao, P. Rinke, and A. S. Foster, *DScribe: Library of descriptors for machine learning in materials science,* Computer Physics Communications **247**, 106949 (2020). doi:10.1016/j.cpc.2019.106949.

[25] Z. Fan, Z. Zeng, C. Zhang, Y. Wang, K. Song, H. Dong, Y. Chen, and T. Ala-Nissila, *Neuroevolution machine learning potentials: Combining high accuracy and low cost in atomistic simulations and application to heat transport,* Phys. Rev. B **104**, 104309 (2021). doi:10.1103/PhysRevB.104.104309.

[26] A. V. Shapeev, *Moment Tensor Potentials: A Class of Systematically Improvable Interatomic Potentials,* Multiscale Modeling & Simulation **14**, 1153 (2016). doi:10.1137/15m1054183.

[27] I. S. Novikov, K. Gubaev, E. V. Podryabinkin, and A. V. Shapeev, *The MLIP package: moment tensor potentials with MPI and active learning,* Machine Learning: Science and Technology **2**, 025002 (2021). doi:10.1088/2632-2153/abc9fe.

[28] F. Pedregosa, G. Varoquaux, A. Gramfort, V. Michel, B. Thirion, O. Grisel, M. Blondel, P. Prettenhofer, R. Weiss, V. Dubourg, J. Vanderplas, A. Passos, D. Cournapeau, M. Brucher, M. Perrot, and E. Duchesnay, *Scikit-learn: Machine Learning in Python,* Journal of Machine Learning Research **12**, 2825 (2011).

[29] M. Karabin and D. Perez, *An entropy-maximization approach to automated training set generation for interatomic potentials,* The Journal of Chemical Physics **153**, 094110 (2020). doi:10.1063/5.0013059.

[30] Y. Zuo, C. Chen, X. Li, Z. Deng, Y. Chen, J. Behler, G. Csányi, A. V. Shapeev, A. P. Thompson, M. A. Wood, and S. P. Ong, *Performance and Cost Assessment of Machine Learning Interatomic Potentials,* The Journal of Physical Chemistry A **124**, 731 (2020). doi:10.1021/acs.jpca.9b08723.

[31] D. Frenkel and B. Smit, *Understanding Molecular Simulation: From Algorithms to Applications* (Academic Press, 1996).

[32] M. Ceriotti, J. More, and D. E. Manolopoulos, *i-PI: A Python interface for ab initio path integral molecular dynamics simulations,* Computer Physics Communications **185**, 1019 (2014). doi:10.1016/j.cpc.2013.10.027.

[33] G. Bussi, D. Donadio, and M. Parrinello, *Canonical sampling through velocity rescaling,* The Journal of Chemical Physics **126**, 014101 (2007). doi:10.1063/1.2408420.

[34] A. P. Thompson, S. J. Plimpton, and W. Mattson, *General formulation of pressure and stress tensor for arbitrary many-body interaction potentials under periodic boundary conditions,* The Journal of Chemical Physics **131**, 154107 (2009). doi:10.1063/1.3245303.

[35] E. Fransson and P. Erhart, *Defects from phonons: Atomic transport by concerted motion in simple crystalline metals,* Acta Materialia **196**, 770 (2020). doi:10.1016/j.actamat.2020.06.040.

[36] E. Fransson, M. Slabanja, P. Erhart, and G. Wahnström, *dynasor—A Tool for Extracting Dynamical Structure Factors and Current Correlation Functions from Molecular Dynamics Simulations,* Advanced Theory and Simulations **4**, 2000240 (2021). doi:10.1002/adts.202000240.

[37] A. Carreras, A. Togo, and I. Tanaka, *DynaPhoPy: A code for extracting phonon quasiparticles from molecular dynamics simulations,* Computer Physics Communications **221**, 221 (2017). doi:10.1016/j.cpc.2017.08.017.

[38] R. Fair, A. Jackson, D. Voneshen, D. Jochym, D. Le, K. Refson, and T. Perring, *Euphonic: inelastic neutron scattering simulations from force constants and visualisation tools for phonon properties,* 2022. doi:10.48550/arxiv.2206.15289.

[39] M. Born and K. Huang, *Dynamical Theory of Crystal Lattices* (Oxford University Press, 1998). ISBN 0198503695.

[40] J. M. Ziman, *Electrons and Phonons* (Oxford University Press, London, 1960).

[41] P. Choquard, *The anharmonic crystal* (New York: W. A. Benjamin, Inc., 1967).

[42] D. C. Wallace, *Thermodynamics of Crystals* (Dover Publications, 1998). ISBN 0-486-40212-6.

[43] G. P. Srivastava, *The physics of phonons* (New York: Taylor and Francis Group, 1990).

[44] A. Togo and I. Tanaka, *Spglib: a software library for crystal symmetry search,* 2018. doi:10.48550/ARXIV.1808.01590.

[45] J. Carrete, W. Li, L. Lindsay, D. A. Broido, L. J. Gallego, and N. Mingo, *Physically founded phonon dispersions of few-layer materials and the case of borophene,* Materials Research Letters **4**, 204 (2016). doi:10.1080/21663831.2016.1174163.

[46] K. Esfarjani and H. T. Stokes, *Method to extract anharmonic force constants from first principles calculations,* Phys. Rev. B **77**, 144112 (2008). doi:10.1103/PhysRevB.77.144112.

[47] P. Giannozzi, S. de Gironcoli, P. Pavone, and S. Baroni, *Ab initio calculation of phonon dispersions in semiconductors,* Phys. Rev. B **43**, 7231 (1991). doi:10.1103/PhysRevB.43.7231.

[48] R. M. Pick, M. H. Cohen, and R. M. Martin, *Microscopic Theory of Force Constants in the Adiabatic Approximation,* Phys. Rev. B **1**, 910 (1970). doi:10.1103/PhysRevB.1.910.

[49] X. Gonze and C. Lee, *Dynamical matrices, Born effective charges, dielectric permittivity tensors, and interatomic force constants from density-functional perturbation theory,* Phys. Rev. B **55**, 10355 (1997). doi:10.1103/PhysRevB.55.10355.

[50] X. Gonze and C. Lee, *Dynamical matrices, Born effective charges, dielectric permittivity tensors, and interatomic force constants from density-functional perturbation theory,* Phys. Rev. B **55**, 10355 (1997). doi:10.1103/PhysRevB.55.10355.

[51] K. Parlinski, Z. Q. Li, and Y. Kawazoe, *First-Principles Determination of the Soft Mode in Cubic* ZrO_2, Phys. Rev. Lett. **78**, 4063 (1997). doi:10.1103/PhysRevLett.78.4063.

[52] E. Jedvik, *Vibrational and Structural Characterisation in Two Perovskite Challenges: A Density Functional Theory Study.* PhD thesis, Chalmers University of Technology, 2019.

[53] A. Togo, L. Chaput, and I. Tanaka, *Distributions of phonon lifetimes in Brillouin zones,* Phys. Rev. B **91**, 094306 (2015). doi:10.1103/PhysRevB.91.094306.

[54] T. Tadano, Y. Gohda, and S. Tsuneyuki, *Anharmonic force constants extracted from first-principles molecular dynamics: applications to heat transfer simulations,* Journal of Physics: Condensed Matter **26**, 225402 (2014). doi:10.1088/0953-8984/26/22/225402.

[55] W. Li, J. Carrete, N. A. Katcho, and N. Mingo, *ShengBTE: a solver of the Boltzmann transport equation for phonons,* Comp. Phys. Commun. **185**, 1747–1758 (2014). doi:10.1016/j.cpc.2014.02.015.

[56] T. Feng, L. Lindsay, and X. Ruan, *Four-phonon scattering significantly reduces intrinsic thermal conductivity of solids,* Phys. Rev. B **96**, 161201 (2017). doi:10.1103/PhysRevB.96.161201.

[57] T. Tadano and S. Tsuneyuki, *Self-consistent phonon calculations of lattice dynamical properties in cubic* $SrTiO_3$ *with first-principles anharmonic force constants,* Phys. Rev. B **92**, 054301 (2015). doi:10.1103/PhysRevB.92.054301.

[58] Y. Oba, T. Tadano, R. Akashi, and S. Tsuneyuki, *First-principles study of phonon anharmonicity and negative thermal expansion in* ScF_3, Phys. Rev. Materials **3**, 033601 (2019). doi:10.1103/PhysRevMaterials.3.033601.

[59] K. Esfarjani and Y. Liang, *Thermodynamics of anharmonic lattices from first principles,* in *Nanoscale Energy Transport* (IOP Publishing, 2020), p. 7. doi:10.1088/978-0-7503-1738-2ch7.

[60] A. Togo and I. Tanaka, *First principles phonon calculations in materials science,* Scripta Materialia **108**, 1 (2015). doi:10.1016/j.scriptamat.2015.07.021.

[61] W. Li, L. Lindsay, D. A. Broido, D. A. Stewart, and N. Mingo, *Thermal conductivity of bulk and nanowire* $Mg_2Si_xSn_{1-x}$ *alloys from first principles,* Phys. Rev. B **86**, 174307 (2012).

[62] D. West and S. K. Estreicher, *Isotope dependence of the vibrational lifetimes of light impurities in Si from first principles,* Phys. Rev. B **75**, 075206 (2007). doi:10.1103/PhysRevB.75.075206.

[63] R. Bianco, I. Errea, L. Paulatto, M. Calandra, and F. Mauri, *Second-order structural phase transitions, free energy curvature, and temperature-dependent anharmonic phonons in the self-consistent harmonic approximation: Theory and stochastic implementation,* Phys. Rev. B **96**, 014111 (2017). doi:10.1103/PhysRevB.96.014111.

[64] I. Errea, M. Calandra, and F. Mauri, *Anharmonic free energies and phonon dispersions from the stochastic self-consistent harmonic approximation: Application to platinum and palladium hydrides,* Phys. Rev. B **89**, 064302 (2014). doi:10.1103/PhysRevB.89.064302.

[65] L. Monacelli, I. Errea, M. Calandra, and F. Mauri, *Pressure and stress tensor of complex anharmonic crystals within the stochastic self-consistent harmonic approximation,* Phys. Rev. B **98**, 024106 (2018). doi:10.1103/PhysRevB.98.024106.

[66] L. Monacelli, R. Bianco, M. Cherubini, M. Calandra, I. Errea, and F. Mauri, *The stochastic self-consistent harmonic approximation: calculating vibrational properties of materials with full quantum and anharmonic effects,* Journal of Physics: Condensed Matter **33**, 363001 (2021). doi:10.1088/1361-648x/ac066b.

[67] I. Errea, M. Calandra, and F. Mauri, *First-Principles Theory of Anharmonicity and the Inverse Isotope Effect in Superconducting Palladium-Hydride Compounds,* Phys. Rev. Lett. **111**, 177002 (2013). doi:10.1103/PhysRevLett.111.177002.

[68] O. Hellman, I. A. Abrikosov, and S. I. Simak, *Lattice dynamics of anharmonic solids from first principles,* Phys. Rev. B **84**, 180301 (2011). doi:10.1103/PhysRevB.84.180301.

[69] O. Hellman and I. A. Abrikosov, *Temperature-dependent effective third-order interatomic force constants from first principles,* Phys. Rev. B **88**, 144301 (2013). doi:10.1103/PhysRevB.88.144301.

[70] O. Hellman, P. Steneteg, I. A. Abrikosov, and S. I. Simak, *Temperature dependent effective potential method for accurate free energy calculations of solids,* Phys. Rev. B **87**, 104111 (2013). doi:10.1103/PhysRevB.87.104111.

[71] D. O. Lindroth, J. Brorsson, E. Fransson, F. Eriksson, A. Palmqvist, and P. Erhart, *Thermal conductivity in intermetallic clathrates: A first-principles perspective,* Physical Review B **100**, 045206 (2019). doi:10.1103/PhysRevB.100.045206.

[72] F. Zhou, W. Nielson, Y. Xia, and V. Ozoliņš, *Lattice Anharmonicity and Thermal Conductivity from Compressive Sensing of First-Principles Calculations,* Phys. Rev. Lett. **113**, 185501 (2014). doi:10.1103/PhysRevLett.113.185501.

[73] J. Brorsson, A. Hashemi, Z. Fan, E. Fransson, F. Eriksson, T. Ala-Nissila, A. V. Krasheninnikov, H.-P. Komsa, and P. Erhart, *Efficient Calculation of the Lattice Thermal Conductivity by Atomistic Simulations with Ab Initio Accuracy,* Advanced Theory and Simulations **5**, 2100217 (2022). doi:10.1002/adts.202100217.

[74] F. Zhou, W. Nielson, Y. Xia, and V. Ozoliņš, *Compressive sensing lattice dynamics. I. General formalism,* Phys. Rev. B **100**, 184308 (2019). doi:10.1103/PhysRevB.100.184308.

[75] F. Zhou, B. Sadigh, D. Åberg, Y. Xia, and V. Ozoliņš, *Compressive sensing lattice dynamics. II. Efficient phonon calculations and long-range interactions,* Phys. Rev. B **100**, 184309 (2019). doi:10.1103/PhysRevB.100.184309.

[76] E. Fransson, *Atomic-scale investigation of interfacial structures in WC-Co at finite temperatures.* PhD thesis, Chalmers university of technology, 2021.

[77] R. Peierls, *Zur kinetischen Theorie der Wärmeleitung in Kristallen,* Annalen der Physik **395**, 1055 (1929). doi:10.1002/andp.19293950803.

[78] W. Li, N. Mingo, L. Lindsay, D. A. Broido, D. A. Stewart, and N. A. Katcho, *Thermal conductivity of diamond nanowires from first principles,* Phys. Rev. B **85**, 195436 (2012).

[79] Z. Han, X. Yang, W. Li, T. Feng, and X. Ruan, *FourPhonon: An extension module to ShengBTE for computing four-phonon scattering rates and thermal conductivity,* Computer Physics Communications **270**, 108179 (2022). doi:10.1016/j.cpc.2021.108179.

[80] D. Lindroth, *Thermal transport in van der Waals Solids and Inorganic Clathrates from first-principles calculations.* PhD thesis, Chalmers university of technology, 2018.

[81] L. Lindsay, A. Katre, A. Cepellotti, and N. Mingo, *Perspective on ab initio phonon thermal transport,* Journal of Applied Physics **126**, 050902 (2019). doi:10.1063/1.5108651.

[82] L. Chaput, *Direct Solution to the Linearized Phonon Boltzmann Equation,* Phys. Rev. Lett. **110**, 265506 (2013). doi:10.1103/PhysRevLett.110.265506.

[83] M. Simoncelli, N. Marzari, and F. Mauri, *Unified theory of thermal transport in crystals and glasses,* Nature Physics **15**, 809 (2019). doi:/10.1038/s41567-019-0520-x.

[84] M. Simoncelli, N. Marzari, and F. Mauri, *Wigner formulation of thermal transport in solids,* arXiv preprint arXiv:2112.06897 , (2021). https://arxiv.org/abs/2112.06897.

[85] G. Barbalinardo, Z. Chen, N. W. Lundgren, and D. Donadio, *Efficient anharmonic lattice dynamics calculations of thermal transport in crystalline and disordered solids,* Journal of Applied Physics **128**, 135104 (2020).

[86] S. Baroni, R. Bertossa, L. Ercole, F. Grasselli, and A. Marcolongo, *Heat Transport in Insulators from Ab Initio Green-Kubo Theory.* In W. Andreoni and S. Yip, eds., *Handbook of Materials Modeling: Applications: Current and Emerging Materials* (Cham: Springer International Publishing, 2020). doi:10.1007/978-3-319-44680-6_12.

[87] D. J. Evans, *Homogeneous NEMD algorithm for thermal conductivity—Application of noncanonical linear response theory,* Physics Letters A **91**, 457 (1982). doi:10.1016/0375-9601(82)90748-4.

[88] Z. Fan, L. F. C. Pereira, H.-Q. Wang, J.-C. Zheng, D. Donadio, and A. Harju, *Force and heat current formulas for many-body potentials in molecular dynamics simulations with applications to thermal conductivity calculations,* Phys. Rev. B **92**, 094301 (2015). doi:10.1103/PhysRevB.92.094301.

[89] Z. Fan, H. Dong, A. Harju, and T. Ala-Nissila, *Homogeneous nonequilibrium molecular dynamics method for heat transport and spectral decomposition with many-body potentials,* Phys. Rev. B **99**, 064308 (2019). doi:10.1103/PhysRevB.99.064308.

[90] M. Ångqvist, W. A. Muñoz, J. M. Rahm, E. Fransson, C. Durniak, P. Rozyczko, T. H. Rod, and P. Erhart, *ICET – A Python Library for Constructing and Sampling Alloy Cluster Expansions,* Advanced Theory and Simulations **2**, 1900015 (2019). doi:10.1002/adts.201900015.

[91] L. J. Nelson, V. Ozoliņš, C. S. Reese, F. Zhou, and G. L. W. Hart, *Cluster expansion made easy with Bayesian compressive sensing,* Phys. Rev. B **88**, 155105 (2013). doi:10.1103/PhysRevB.88.155105.

[92] F. Zhou, W. Nielson, Y. Xia, and V. Ozolins, *Lattice anharmonicity and thermal conductivity from compressive sensing of first-principles calculations,* Phys. Rev. Lett. **113**, 185501 (2014). doi:10.1103/PhysRevLett.113.185501.

[93] D. O. Lindroth and P. Erhart, *Thermal transport in van der Waals solids from first-principles calculations,* Phys. Rev. B **94**, 115205 (2016). doi:10.1103/PhysRevB.94.115205.

[94] T. Liang, S. R. Phillpot, and S. B. Sinnott, *Parametrization of a reactive many-body potential for Mo–S systems,* Phys. Rev. B **79**, 245110 (2009). doi:10.1103/PhysRevB.79.245110.

[95] Z. Fan, T. Siro, and A. Harju, *Accelerated molecular dynamics force evaluation on graphics processing units for thermal conductivity calculations,* Computer Physics Communications **184**, 1414 (2013). doi:10.1016/j.cpc.2013.01.008.

[96] S. Curtarolo, G. L. W. Hart, M. B. Nardelli, N. Mingo, S. Sanvito, and O. Levy, *The high-throughput highway to computational materials design.,* Nature Materials **12**, 191–201 (2013). doi:10.1038/nmat3568.

[97] R. Jinnouchi, K. Miwa, F. Karsai, G. Kresse, and R. Asahi, *On-the-Fly Active Learning of Interatomic Potentials for Large-Scale Atomistic Simulations,* The Journal of Physical Chemistry Letters **11**, 6946 (2020). PMID: 32787192. doi:10.1021/acs.jpclett.0c01061.

[98] Z. Fan, Y. Wang, P. Ying, K. Song, J. Wang, Y. Wang, Z. Zeng, K. Xu, E. Lindgren, J. M. Rahm, A. J. Gabourie, J. Liu, H. Dong, J. Wu, Y. Chen, Z. Zhong, J. Sun, P. Erhart, Y. Su, and T. Ala-Nissila, *GPUMD: A package for constructing accurate machine-learned potentials and performing highly efficient atomistic simulations,* 2022. doi:10.48550/ARXIV.2205.10046.

[99] C. Carbogno, R. Ramprasad, and M. Scheffler, *Ab Initio Green-Kubo Approach for the Thermal Conductivity of Solids,* Phys. Rev. Lett. **118**, 175901 (2017). doi:10.1103/PhysRevLett.118.175901.

[100] F. Knoop, *Heat transport in strongly anharmonic solids from first principles.* PhD thesis, Humboldt-Universität zu Berlin, Mathematisch-Naturwissenschaftliche Fakultät, 2022. doi:http://dx.doi.org/10.18452/24244.